

Caching Policy Toward Maximal Success Probability and Area Spectral Efficiency of Cache-enabled HetNets

Dong Liu and Chenyang Yang

Abstract

In this paper, we investigate the optimal caching policy respectively maximizing the success probability and area spectral efficiency (ASE) in a cache-enabled heterogeneous network (HetNet) where a tier of multi-antenna macro base stations (MBSs) is overlaid with a tier of helpers with caches. Under the probabilistic caching framework, we resort to stochastic geometry theory to derive the success probability and ASE. After finding the optimal caching policies, we analyze the impact of critical system parameters and compare the ASE with traditional HetNet where the MBS tier is overlaid by a tier of pico BSs (PBSs) with limited-capacity backhaul. Analytical and numerical results show that the optimal caching probability is less skewed among helpers to maximize the success probability when the ratios of MBS-to-helper density, MBS-to-helper transmit power, user-to-helper density, or the rate requirement are small, but is more skewed to maximize the ASE in general. Compared with traditional HetNet, the helper density is much lower than the PBS density to achieve the same target ASE. The helper density can be reduced by increasing cache size. With given total cache size within an area, there exists an optimal helper node density that maximizes the ASE.

Index Terms

Caching policy, area spectral efficiency, success probability, heterogeneous networks

I. INTRODUCTION

To support the 1000-fold higher throughput in the fifth-generation (5G) cellular systems, a promising way is to densify the network by deploying more small base stations (BSs) in a macro

The authors are with School of Electronics and Information Engineering, Beihang University, Beijing, China (e-mail: {dliu, cyyang}@buaa.edu.cn). Parts of this work were published in IEEE ICC 2016 [1] and to be presented at IEEE GLOBECOM 2016 [2].

cell [3]. Such heterogeneous networks (HetNets) can offload the traffic and increase the area spectral efficiency (ASE), but the gain largely relies on high-speed backhaul links. Although optical fiber can provide high capacity, bringing fiber-connection to every single small BS is rather labor-intensive and expensive. Alternatively, digital subscriber line (DSL) or microwave backhaul may easily become a bottleneck and frustratingly impair the throughput gain brought by the network densification [4].

Recently, it has been observed that a large portion of mobile data traffic is generated by many duplicate downloads of a few popular contents [5]. Besides, the storage capacity of today's memory devices grows rapidly at a relatively low cost. Motivated by these facts, the authors in [6] suggested to replace small BSs by the BSs that have weak backhaul links (or even completely without backhaul) but have high capacity caches, called *helper nodes*. By optimizing the caching policies to serve more users under the constraints of file downloading time, large throughput gain was reported. Considering small cell networks (SCNs) with backhaul of very limited capacity, the authors in [7] observed that the backhaul traffic load can be reduced by caching files at the small BSs based on their popularity. These results indicate that by fetching contents locally instead of fetching from core network via backhaul links duplicately, equipping caches at BSs is a promising way to unleash the potential of HetNet.

In [8], both the throughput and energy efficiency of homogeneous cached-enabled cellular networks with hexagonal cells were analyzed. For HetNets or SCNs, however, it is more appropriate to use Poisson Point Process (PPP) to model the BS location [9]. Stochastic geometry theory was first applied in [10] for a homogeneous cache-enabled SCN where average delivery rate was derived by assuming that the delivery rate is a constant when channel capacity exceeds a threshold. In [11], the throughput of a cache-enabled network with content pushing to users, device-to-device communication and caching at relays was derived, where every node (including the macro BS (MBS) and relay) is with a single antenna and with high-capacity backhaul.

Caching policy is critical in reaping the benefit brought by caching. In [8, 10, 11], the authors considered caching the most popular files at each small-BS. In wireless networks, when the coverage of several BSs overlaps, a user is able to fetch contents from multiple helpers and hence cache-hit probability can be increased by caching different files among helpers [12]. However, owing to interference and path loss, such a file diversity may lead to low signal-to-interference-plus-noise ratio (SINR), since a user may associate with a relative further BS to

“hit the cache” when the nearest BS does not cache the requested file [8].

In [12], caching policy was optimized to minimize the file download time where the interference among helpers are not considered. In [13], the optimal caching policy was proposed to minimize the average bit error rate over fading channels. Both [12] and [13] assume *a priori* known BS-user topology, which is not practical in mobile networks. To reflect the uncertain connectivity between BS and user, a probabilistic caching framework was proposed recently in [14], where the network models based on stochastic geometry were considered that are more realistic tractable. In particular, a probabilistic caching policy was proposed where each BS caches files independently according to an optimized caching probability to maximize the cache-hit probability. However, the optimal caching probability is not obtained with closed-form, which makes it hard to gain useful insights into the impact of various system parameters. In [15], the optimal caching probability maximizing the successful transmission probability in a homogeneous network was obtained in closed-form when user density approaches infinity. In [16], caching policy was optimized to maximize the traffic offloaded to helpers and cache-enabled users, but the links among helpers and users are assumed interference-free. In real-world HetNets, the interference is complicated and has large impact on the system design and network performance. While deploying helpers is a cost-effective way for offloading traffic and increasing ASE of cellular networks, how to place the contents and how to deploy the helpers for interference-limited cache-enabled HetNets are still not well understood. Specifically,

- Existing works rarely consider caching policy optimization in HetNets, and the basic features of cache-enabled HetNets are not well captured and analyzed, such as BS and user densities, rate requirement and association bias.
- Existing works mainly focus on finding the optimal caching probability maximizing the success probability in cache-enabled networks, but never consider caching policy optimization for maximizing the ASE, yet another important performance metric.
- Existing works never consider helper idling, which affects the optimization for caching policy, and is appealing since the cost-effective helpers make dense deployment possible.

In this paper, we attempt to find the optimal caching policy for cache-enabled HetNet under different performance metrics, analyze the impact of critical system parameters, investigate the benefits of cache-enabled HetNet with respect to traditional HetNet with limited-capacity

backhaul, and reveal the tradeoff in deploying cache-enabled HetNets. To this end, we consider a cache-enabled HetNet where a tier of multi-antenna MBSs is overlaid with a tier of denser helpers with caches but without backhaul links. Under the probabilistic caching framework [14] and using stochastic geometry theory, we derive the success probability and ASE of the cache-enabled HetNets respectively as functions of BS/helper node density, user density, caching probability, storage size and file popularity. We also derive the ASE of traditional HetNet where a tier of MBSs is overlaid with a tier of PBS with limited-capacity backhaul for comparison. The major contributions of this paper are summarized as follows,

- We find the optimal caching policy to maximize a concave lower bound of the success probability, which becomes very tight in low user density case. With the optimized caching probability, we analyze the impact of critical system parameters, including user density, BS density, transmit power, rate requirement and association bias factor.
- We find the optimal caching policy to maximize the approximated ASE, which is accurate for small cache size of each helper. When that user-to-helper density and helper-to-MBS density approach infinity, we prove that simply caching the most popular files everywhere is the optimal solution, which is quite different from maximizing the success probability.
- We show that the cache-enabled HetNet can provide much higher ASE than the traditional HetNet with the same PBS/helper density, or can be deployed with much lower helper density than the PBS density of traditional HetNet to achieve the same target ASE, which can reduce the cost of deployment and operation remarkably. Moreover, we find that the helper density can be traded off by the cache size to achieve a target ASE. Given the total cache size within an area, there exists an optimal helper density that maximizes the ASE.

The rest of this paper is organized as follows. In Section II, we present the system model. The caching policies toward maximizing success probability and ASE are optimized in Section III and Section IV, respectively. The numerical and simulation results are provided in Section V, and the conclusions are drawn in Section VI.

II. SYSTEM MODEL

A. Network Model

We consider a cache-enabled HetNet, where a tier of MBSs is overlaid with a tier of denser helper nodes. The MBSs are connected to the core network with high-capacity backhaul links,

e.g., optical fibers, and the helper nodes are deployed without backhaul but equipped with caches.

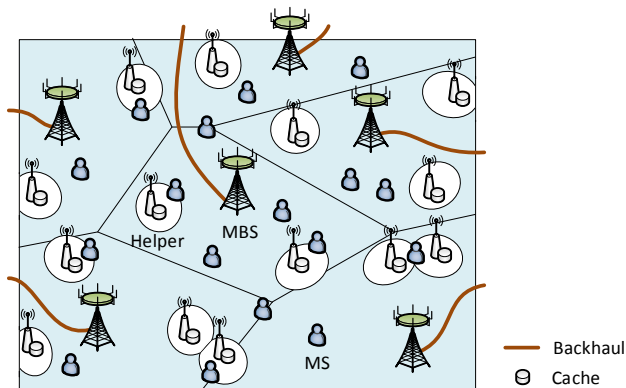


Fig. 1. Layouts of the considered cache-enabled HetNets.

The distribution of MBSs, helper nodes and users are modeled as three independent homogeneous PPPs with density of λ_1 , λ_2 and λ_u , denoted as Φ_1 , Φ_2 and Φ_u , respectively. Each MBS is equipped with $M_1 \geq 1$ antennas and each helper node is with $M_2 = 1$ antenna.¹ Denote $k \in \{1, 2\}$ as the index of the tier that a randomly chosen user in the network (called the typical user) is associated with. In the following, if not specified, BS refers to either MBS or helper. The transmit power at each BS in the k th tier is denoted by P_k .

We assume that each user requests a file from a content catalog that contains N_f files randomly. The files are indexed according to their popularity, ranking from the most popular (the 1st file) to the least popular (the N_f th file). The probability that the f th popular file is requested follows Zipf distribution as

$$p_f = f^{-\delta} / \left(\sum_{n=1}^{N_f} n^{-\delta} \right) \quad (1)$$

where the skew parameter δ is with typical value of $0.5 \sim 1.0$ [17]. For simplicity, we assume that the files are with equal size² and the cache size of each helper node is N_c .

We consider probabilistic caching policy where each helper independently selects files to cache according to a specific probability distribution. To unify the analysis, denote $0 \leq q_{f,k} \leq 1$ as the probability that the BS of the k th tier caches the f th file. When $\mathbf{q}_k \triangleq [q_{f,k}]_{f=1, \dots, N_f}$ is given,

¹Since helper nodes are expected to enable dense deployment with low cost, we only consider single-antenna case.

²Files with different size can be divided into equal-size content chunks.

each BS can determine which files should be cached by the method in [14]. For the MBS tier, $q_1 = 1$, since the MBS can be regarded as caching all the files due to the high-capacity backhaul.

Since every helper caches files independently, the distribution of the BSs in the k th tier that cache the f th file can be regarded as a thinning of the PPP Φ_k with probability $q_{f,k}$, which follows a PPP with density $q_{f,k}\lambda_k$ (denoted by $\Phi_{f,k}$). Similarly, the distribution of the BSs in the k th tier that do not cache the f th file follows PPP with density $(1 - q_{f,k})\lambda_k$ (denoted by $\Phi_{f',k}$).

We consider user association based on both channel condition and cached files in each helper. Specifically, when the typical user requests the f th file, it associates with the BS in the set of $\{\Phi_{f,k}\}_{k=1,2}$ that has the strongest average biased-received-power (BRP). The BRP for the k th tier is $P_{r,k} = P_k B_k r^{-\alpha}$, where $B_k \geq 0$ is the association bias factor, r is the BS-user distance, and α is the path-loss exponent. In such a cache-enabled HetNet, the user may not associate with the BS with the strongest BRP since the BS may not cache the requested file, which is very different from the traditional HetNets.

We assume that $\lambda_u \gg \lambda_1$ such that the number of users in each macro cell far exceeds the number of antennas at each MBS M_1 , and each MBS randomly select M_1 users to serve. Since the helpers without backhaul can be densely deployed at low cost and the traffic may fluctuate among peak and off-peak times, the density of helper nodes may become comparable with the density of users and hence some helpers may have no users to serve. These inactive helpers will become muting, i.e., be turned into idle mode to avoid generating interference. Each MBS serves every M_1 users in the same time-frequency resource by zero-forcing beamforming with equal power allocation, while each helper serves its associated users by time division or frequency division multiple access with full power. These assumptions define a typical scenario, which however can capture the fundamental features of cache-enabled HetNets. Then, the downlink SINR at the typical user that requests the f th file and associates with the k th tier is

$$\begin{aligned} \gamma_{f,k} &= \frac{\frac{P_k}{M_k} h_{k0} r_k^{-\alpha}}{\sum_{j=1}^2 \left(\sum_{i \in \tilde{\Phi}_{f,j} \setminus b_{k0}} P_j h_{ji} r_{ji}^{-\alpha} + \sum_{i \in \tilde{\Phi}_{f',j}} P_j h_{ji} r_{ji}^{-\alpha} \right) + \sigma^2} \\ &\triangleq \frac{\frac{P_k}{M_k} h_{k0} r_k^{-\alpha}}{\sum_{j=1}^2 (I_{f,kj} + I_{f',kj}) + \sigma^2} \triangleq \frac{\frac{P_k}{M_k} h_{k0} r_k^{-\alpha}}{I_k + \sigma^2} \end{aligned} \quad (2)$$

where h_{k0} is the equivalent channel (including channel coefficient and beamforming) from the associated BS b_{k0} to the typical user, r_k is the corresponding distance, $\tilde{\Phi}_{f,j}$ and $\tilde{\Phi}_{f',j}$ are respectively the sets of active BSs in the j th tier that caching and not caching the f th file,

h_{ji} and r_{ji} are the equivalent interference channel and distance from the i th active BS in the j th tier to the typical user, and σ^2 is the noise power. We consider Rayleigh fading channels. Then, h_{k0} follows exponential distribution with unit mean (i.e., $h_{k0} \sim \exp(1)$), and h_{ij} follows gamma distribution with shape parameter M_j and unit mean (i.e., $h_{ij} \sim \mathbb{G}(M_j, 1/M_j)$) [18]. The total interference I_k consists of the interference from the BSs that caching the f th file (denoted by $I_{f,kj}$) and the interference from the BSs that do not cache the f th file (denoted by $I_{f',kj}$).

Since HetNets are usually interference-limited [9], it is reasonable to neglect the thermal noise, i.e., $\sigma^2 = 0$.³ For notational simplicity, we define the ratios of BS density, number of antennas, transmit power, and bias factor as $\lambda_{jk} \triangleq \lambda_j/\lambda_k$, $M_{jk} \triangleq M_j/M_k$, $P_{jk} \triangleq P_j/P_k$, and $B_{jk} \triangleq B_j/B_k$, respectively. Note that $\lambda_{kk} = M_{kk} = P_{kk} = B_{kk} = 1$.

B. Performance Metric

We consider two performance metrics, either from each user or the network perspective.

From the user perspective, we use success probability to reflect the quality of service, which is the probability that the achievable rate of the typical user exceeds the rate requirement R_0 . Since we assume $\lambda_u \gg \lambda_1$ and M_1 is not large, when the user associates with the MBS, the time-frequency resources allocated to the user could be too stringent to support the rate requirement. Therefore, we define the success probability as the probability that the typical user associates with the helper tier and with achievable rate higher than R_0 , which can be expressed as

$$p_s \triangleq \mathbb{P} \left(\frac{W}{U_k/M_k} \log_2(1 + \gamma_k) \geq R_0, k = 2 \right) = \mathbb{P}(\gamma_k \geq \gamma_0, k = 2) \quad (3)$$

where W is the total transmission bandwidth of the network, U_k is the number of users served by the same BS together with the typical user, and \mathbb{P} denotes the probability. Since each BS serves M_k users on the same time-frequency resource, $\frac{W}{U_k/M_k}$ represents the time-frequency resource allocated to each user, and $\gamma_0 \triangleq 2^{\frac{R_0 U_k}{W M_k}} - 1$ is the equivalent per-user SINR requirement.

From the network perspective, we use ASE to measure the network capacity, which is defined as the average throughput per unit area normalized by the transmission bandwidth [19],

$$\text{ASE} = \frac{1}{W} \sum_{k=1}^2 p_{a,k} \lambda_k \mathbb{E}[R_k] \quad (4)$$

³The analysis can be extended to the case when $\sigma^2 \neq 0$, but closed-form expression cannot be obtained.

where $p_{a,k}$ is the probability that a randomly chosen BS in the k th tier is active, R_k is the throughput of the active BS in the k th tier, and \mathbb{E} denotes the expectation. The expectation is taken over file requests, cached files among helpers, the number and location of BSs and users, and small-scale fading.

III. CACHING POLICY MAXIMIZING SUCCESS PROBABILITY

In this section, we first derive the success probability as a function of caching probability, then find the optimal caching probability maximizing the success probability and analyze the impact of different system settings on the optimal caching policy.

A. Successful Probability

To derive the main results, we first introduce a lemma regarding the tier association probability.

Lemma 1: The probability of the typical user associating with the k th tier is

$$\mathcal{P}_k(\mathbf{q}_2) = \sum_{f=1}^{N_f} \frac{p_f q_{f,k}}{\sum_{j=1}^2 q_{f,j} \lambda_{jk} (P_{jk} B_{jk})^{\frac{2}{\alpha}}} \quad (5)$$

and the probability of the typical user associating with the k th tier conditioned on that the user requests the f th file is

$$\mathcal{P}_{f,k}(\mathbf{q}_2) = q_{f,k} \left(\sum_{j=1}^2 q_{f,j} \lambda_{jk} (P_{jk} B_{jk})^{\frac{2}{\alpha}} \right)^{-1} \quad (6)$$

Proof: See Appendix A. ■

Since $\mathcal{P}_{f,k}(\mathbf{q}_2)$ increases with $q_{f,k}$, with more BSs in the k th tier caching the f th file, the user requesting the f th file is more likely to associate with the k th tier. For notational simplicity, in the following we denote $\mathcal{P}_k(\mathbf{q}_2)$ and $\mathcal{P}_{f,k}(\mathbf{q}_2)$ as \mathcal{P}_k and $\mathcal{P}_{f,k}$ for short, respectively.

Then, based on the tier association probability and the downlink SINR distribution, we obtain the success probability in the following proposition.

Proposition 1: The success probability of the typical user is

$$p_s(\mathbf{q}_2) = \sum_{f=1}^{N_f} \frac{p_f q_{f,2}}{C_{1,\gamma_0} + C_{2,\gamma_0} p_{a,2} + C_{3,\gamma_0} p_{a,2} q_{f,2} + q_{f,2}} \quad (7)$$

where $C_{1,\gamma_0} \triangleq \lambda_{12} (P_{12} B_{12})^{\frac{2}{\alpha}} {}_2F_1 \left[-\frac{2}{\alpha}, M_1; 1 - \frac{2}{\alpha}; -\frac{\gamma_0}{M_{12} B_{12}} \right]$, $C_{2,\gamma_0} \triangleq \Gamma(1 - \frac{2}{\alpha}) \Gamma(M_2 + \frac{2}{\alpha_2}) \Gamma(M_2)^{-1} \gamma_0^{\frac{2}{\alpha}}$, $C_{3,\gamma_0} \triangleq {}_2F_1 \left[-\frac{2}{\alpha}, M_2; 1 - \frac{2}{\alpha}; -\gamma_0 \right] - C_{2,\gamma_0} - 1$, $\gamma_0 \approx 2^{\frac{R_0}{W}} \left(1 + \frac{1.28 \lambda_u P_2}{\lambda_2} \right) - 1$ is the equivalent per-user

receive SINR requirement, and $p_{a,2} \approx 1 - \left(1 + \frac{\mathcal{P}_2 \lambda_u}{3.5 \lambda_2}\right)^{-3.5}$ is the probability that a randomly chosen helper is active (i.e., has user associated with), which is accurate when $\lambda_2 \gg \lambda_1$, ${}_2F_1[\cdot]$ and $\Gamma(\cdot)$ denote the Gauss hypergeometric function and Gamma function, respectively.

Proof: See Appendix B. ■

It is shown that the success probability $p_s(\mathbf{q}_2)$ decreases with the helper active probability $p_{a,2}$. This indicates if a helper can be turn into idle mode when no user associates with it (i.e., $p_{a,2} < 1$), the success probability is higher than that without helper idling (i.e., $p_{a,2} = 1$). Proposition 1 also shows that $p_{a,2}$ and γ_0 increase with λ_u . Further considering that $p_s(\mathbf{q}_2)$ decreases with γ_0 as shown in (3), the success probability decreases with user density.

B. Optimal Caching Policy

The optimal caching probability that maximizes the success probability can be found from

$$\begin{aligned} \text{Problem 1: } \quad & \max_{\mathbf{q}_2} p_s(\mathbf{q}_2) \\ & s.t. \quad \sum_{i=1}^{N_f} q_{f,2} \leq N_c \end{aligned} \quad (8a)$$

$$0 \leq q_{f,2} \leq 1, \quad f = 1, \dots, N_f \quad (8b)$$

where (8a) is equivalent to the cache size constraint (i.e., the number of cached file cannot exceed the cache size) for each helper as proved in [14], and (8b) is the probability constraint.

In the following we first solve Problem 1 in general case, and then analyze the behavior of optimal caching policy and the impacts of system settings in high and low user density cases.

1) *General Case:* This problem is not concave in general, because both $p_{a,2}$ and γ_0 in the objective function depend on \mathcal{P}_2 , which is a complicated function of \mathbf{q}_2 as shown in (5). Therefore, only a local optimal solution can be found, say by using interior point method [20]. Such a solution is not only of high complexity when the dimension of optimization variable \mathbf{q}_2 , i.e., N_f , is large, but also hard to provide design guideline for practical systems. In the sequel, we strive to obtain closed-form caching probability. To this end, we first obtain a concave lower-bound of the success probability (denoted as \underline{p}_s) and then solve the problem maximizing \underline{p}_s , which is a concave problem.

Considering that it is the complicated expression of \mathcal{P}_2 as a function of \mathbf{q}_2 that makes the problem non-concave, we introduce a \mathbf{q}_2 -independent upper bound for the probability of

associating with the helper tier \mathcal{P}_2 (denoted by $\bar{\mathcal{P}}_2$), which yields an upper bound for $p_{a,2}$ (denoted by $\bar{p}_{a,2}$) and γ_0 (denoted by $\bar{\gamma}_0$) respectively because $p_{a,2}$ and γ_0 increase with \mathcal{P}_2 as shown in Proposition 1. With $\bar{p}_{a,2}$ and $\bar{\gamma}_0$, we can obtain a lower bound of p_s (denoted by \underline{p}_s) since p_s decreases with $p_{a,2}$ as shown in (7) and decreases with γ_0 as shown in (3).

To obtain a \mathbf{q}_2 -independent upper bound for \mathcal{P}_2 , we first find the optimal caching probability that maximizes \mathcal{P}_2 , denoted as $\mathbf{q}_2^o \triangleq [q_{f,2}^o]_{f=1,\dots,N_f}$. Then, for any \mathbf{q}_2 satisfying (8a) and (8b), $\mathcal{P}_2 \leq \bar{\mathcal{P}}_2$. From Lemma 1 and $\mathbf{q}_1 = \mathbf{1}$, the problem of maximizing \mathcal{P}_2 can be formulated as

$$\begin{aligned} \text{Problem 2: } \max_{\mathbf{q}_2} \mathcal{P}_2 &= \sum_{f=1}^{N_f} \frac{p_f q_{f,2}}{\lambda_{12}(P_{12}B_{12})^{2/\alpha} + q_{f,2}} \\ &s.t. \text{ (8a), (8b)} \end{aligned} \quad (9)$$

It can be easily proved that the Hessian matrix of \mathcal{P}_2 with respect to \mathbf{q}_2 is negative definite. Further considering that constraints (8a) and (8b) are linear, Problem 2 is concave. Then, from the Karush-Kuhn-Tucker (KKT) condition, we obtain the optimal solution of Problem 2 as

$$q_{f,2}^o = \left[\sqrt{\frac{\lambda_{12}(P_{12}B_{12})^{2/\alpha}}{\mu}} \sqrt{p_f} - \lambda_{12}(P_{12}B_{12})^{\frac{2}{\alpha}} \right]_0^1 \quad (10)$$

where $[x]_0^1 = \max\{\min\{x, 1\}, 0\}$ denotes that x is truncated by 0 and 1, and the Lagrange multiplier μ satisfying $\sum_{f=1}^{N_f} q_{f,2}^o = N_c$ can be efficiently found by bisection searching.

By substituting \mathbf{q}_2^o into (9), we can obtain $\bar{\mathcal{P}}_2$. Then, by substituting $\bar{\mathcal{P}}_2$ into (7), we can obtain the lower bound of success probability as

$$\underline{p}_s(\mathbf{q}_2) = \sum_{f=1}^{N_f} \frac{p_f q_{f,2}}{\mathbf{C}_{1,\bar{\gamma}_0} + \bar{p}_{a,2} \mathbf{C}_{2,\bar{\gamma}_0} + (\bar{p}_{a,2} \mathbf{C}_{3,\bar{\gamma}_0} + 1) q_{f,2}} \quad (11)$$

Proposition 2: The optimal caching probability that maximizes the lower bound of the success probability $\underline{p}_s(\mathbf{q}_2)$ is

$$\underline{q}_{f,2}^* = \left[\frac{\sqrt{\mathbf{C}_{1,\bar{\gamma}_0} + \bar{p}_{a,2} \mathbf{C}_{2,\bar{\gamma}_0}}}{\sqrt{\nu}(\bar{p}_{a,2} \mathbf{C}_{3,\bar{\gamma}_0} + 1)} \sqrt{p_f} - \frac{\mathbf{C}_{1,\bar{\gamma}_0} + \bar{p}_{a,2} \mathbf{C}_{2,\bar{\gamma}_0}}{\bar{p}_{a,2} \mathbf{C}_{3,\bar{\gamma}_0} + 1} \right]_0^1 \quad (12)$$

where ν satisfying $\sum_{f=1}^{N_f} \underline{q}_{f,2}^* = N_c$ can be found by bisection searching.

Proof: Since $\bar{p}_{a,2}$ and $\bar{\gamma}_0$ do not depend on $q_{f,2}$, (11) has the same function structure as (9) and hence is a concave function. Then, by using the KKT condition similar to solving Problem 2, we obtain (12). ■

As shown in (12), $\underline{q}_{f,2}^*$ is non-increasing with f since p_f decreases with f , which coincides with the intuition that the file with higher popularity should be cached with higher probability. Moreover, since $\underline{q}_{f,2}^*$ is truncated by 0 and 1, there may exist some files of high popularity (e.g. $f = 1, \dots, N_1$, $N_1 \leq N_f$) with caching probability of 1 (i.e., cached everywhere), and some files of low popularity (e.g. $f = N_f - N_0 + 1, \dots, N_f$, $N_0 \leq N_f - N_1 + 1$) with caching probability of 0 (i.e., not cached at all helpers). For $\underline{q}_{f,2}^* \in (0, 1)$, considering (1), the relation between caching probability and file popularity rank in (12) obeys a shifted power law with exponent $-\delta/2$, which is very different from the noise-limited scenario considered in [16].

Later, we show that the lower bound is tight (i.e., $\underline{p}_s = p_s$) in low user density case. In Section V, we will show that the caching probability $\underline{q}_{f,2}^*$ can achieve almost the same success probability as the caching probability $q_{f,2}^*$ found by inter-point method in general case. Since the computation of $\underline{q}_{f,2}^*$ only requires twice bisection searches on two scalars, i.e., μ and ν , it can be obtained with much lower complexity than the interior point method when N_f is large.

Based on (12), we can analyze the impact of user density on the optimal caching policy.

Corollary 1: For any $\underline{q}_{f,2}^*, \underline{q}_{f+1,2}^* \in (0, 1)$, $\underline{q}_{f,2}^* - \underline{q}_{f+1,2}^*$ increases with λ_u/λ_2 .

Proof: See Appendix C. ■

Corollary 1 indicates that when the ratio of user-to-helper density increases, the files with higher popularity have more chances to be cached and *vice versa*, which reflects a trend towards caching the most popular files everywhere. On the contrary, when the ratio reduces, say from $\lambda_u/\lambda_2 \rightarrow \infty$ (implies no BS idling) to finite values (implies with BS idling), $\underline{q}_{f,2}^* - \underline{q}_{f+1,2}^*$ decreases. This indicates that BS idling makes the caching probability distribution less skewed, i.e., the diversity of cached files increases.

To further analyze how the per-user data rate requirement, BS density and transmit power of different tiers affect the caching policy, we derive the following corollaries in extreme cases.

2) *High user density* ($\lambda_u/\lambda_2 \rightarrow \infty$) : In this case, $p_{a,2} \rightarrow 1$, i.e., all the helpers are active. The lower bound of success probability becomes

$$\underline{p}_s(\mathbf{q}_2) = \sum_{f=1}^{N_f} \frac{p_f q_{f,2}}{\mathbf{C}_{1,\bar{\gamma}_0} + (\mathbf{C}_{3,\bar{\gamma}_0} + 1)q_{f,2}} \quad (13)$$

Similar to deriving (12), we can obtain the optimal caching probability maximizing \underline{p}_s for $\lambda_u/\lambda_2 \rightarrow \infty$ as

$$\underline{q}_{f,2}^* = \left[\frac{\sqrt{C_{1,\bar{\gamma}_0} + C_{2,\bar{\gamma}_0}}}{\sqrt{\nu}(C_{3,\bar{\gamma}_0} + 1)} \sqrt{p_f} - \frac{C_{1,\bar{\gamma}_0} + C_{2,\bar{\gamma}_0}}{C_{3,\bar{\gamma}_0} + 1} \right]_0^1 \quad (14)$$

where the Lagrange multiplier ν satisfying $\sum_{f=1}^{N_f} \underline{q}_{f,2}^* = N_c$ can be found by bisection searching.

Corollary 2: When $R_0 \rightarrow \infty$, $\underline{q}_{1,2}^*, \dots, \underline{q}_{N_c,2}^* = 1$ and $\underline{q}_{N_c+1,2}^*, \dots, \underline{q}_{N_f,2}^* = 0$.

Proof: See Appendix D. ■

Corollary 2 indicates that when the data requirement R_0 is high, the optimal caching policy is simply caching the most popular files everywhere.

3) *Low user density* ($\lambda_u/\lambda_2 \rightarrow 0$): When the user density is low, such that each helper serves at most one user, i.e., $U_2 \rightarrow 1$, and most of helpers have no user to serve, i.e., $p_{a,2} \rightarrow 0$, the success probability can be simplified into

$$p_s(\mathbf{q}_2) = \sum_{f=1}^{N_f} \frac{p_f q_{f,2}}{C_{1,\gamma_0} + q_{f,2}} \quad (15)$$

where $\gamma_0 = 2^{R_0/W} - 1$ because $U_2 \rightarrow 1$. Then, we have $\gamma_0 = \bar{\gamma}_0$ and $p_{a,2} = \bar{p}_{a,2}$ and hence $\underline{p}_s = p_s$, i.e. the lower bound is tight. Note that since γ_0 does not depend on \mathbf{q}_2 anymore in this case, $p_s(\mathbf{q}_2)$ is a concave function and hence Problem 1 becomes concave.

Again, similar to deriving (12), we can obtain the optimal caching probability maximizing p_s for $\lambda_u/\lambda_2 \rightarrow 0$ as

$$q_{f,2}^* = \left[\sqrt{\frac{C_{1,\gamma_0}}{\nu}} \sqrt{p_f} - C_{1,\gamma_0} \right]_0^1 \quad (16)$$

where ν satisfying $\sum_{f=1}^{N_f} q_{f,2}^* = N_c$ can be found by bisection searching. We can prove that the conclusions in Corollary 2 also hold in this case, which are not shown for conciseness.

In the following corollary, we show the impact of BS density and transmit power of different tiers on the caching policy.

Corollary 3: For any $q_{f,2}^*, q_{f+1,2}^* \in (0, 1)$, $q_{f,2}^* - q_{f+1,2}^*$ increases with λ_{12} and P_{12} .

Proof: See Appendix E. ■

Corollary 3 indicates that when the MBS-to-helper density ratio λ_1/λ_2 or MBS-to-helper transmit power ratio P_1/P_2 increases, the files with higher popularity have more chances to be cached while the files with lower popularity have less chances to be cached, leading to a trend

towards caching the most popular files everywhere. By contrast, when λ_1/λ_2 or P_1/P_2 decreases, the caching probability should be less skewed, i.e., the diversity of cached files increases.

IV. CACHING POLICY MAXIMIZING AREA SPECTRAL EFFICIENCY

In this section, we first derive the ASE of the cache-enabled HetNet as a function of caching probability and find the optimal caching probability maximizing the ASE. Then, we explain the difference of the optimal caching probability maximizing the success probability and the ASE. Finally, to show the merit of cache-enabled HetNet, we derived the ASE of traditional HetNets equipped with limited-capacity backhaul for numerical comparison.⁴ In the following, the ASE is computed in units of nats/s/Hz with 1 nat/s = 1.443 bps to simplify the expressions and analysis.

A. Cache-enabled HetNets

Proposition 3: The ASE of the cache-enabled HetNet with different association bias factor in the two tiers is

$$\text{ASE}(\mathbf{q}_2) = \sum_{k=1}^2 \lambda_k p_{a,k} M_k \sum_{f=1}^{N_f} \frac{p_f q_{f,k}}{\mathcal{P}_k} \int_0^\infty \left(\sum_{j=1}^2 \lambda_{jk} P_{jk}^{\frac{2}{\alpha}} \left(q_{f,j} p_{a,j} B_{jk}^{\frac{2}{\alpha}} Z_{1,jk}(e^x - 1) + (1 - q_{f,j}) p_{a,j} Z_{2,jk}(e^x - 1) + q_{f,j} B_{jk}^{\frac{2}{\alpha}} \right) \right)^{-1} dx \quad (17)$$

where $Z_{1,kj}(\gamma_0) \triangleq {}_2F_1\left[-\frac{2}{\alpha}, M_j; 1 - \frac{2}{\alpha}; -\frac{e^x - 1}{M_{jk} B_{jk}}\right] - 1$, and $Z_{2,kj}(\gamma_0) \triangleq \Gamma\left(1 - \frac{2}{\alpha}\right) \Gamma\left(M_j + \frac{2}{\alpha}\right) \times \Gamma(M_j)^{-1} \left(\frac{e^x - 1}{M_{jk}}\right)^{\frac{2}{\alpha}}$.

Proof: See Appendix F. ■

Then, considering the constraints on caching probability and cache size, the caching policy maximizing the ASE of cache-enabled HetNet can be found from

$$\begin{aligned} \text{Problem 3: } \quad & \max_{\mathbf{q}_2} \text{ASE}(\mathbf{q}_2) & (18) \\ & s.t. \quad (8a), (8b) \end{aligned}$$

The computation of ASE requires $2N_f$ numerical integral coupled with \mathbf{q}_k , and hence the optimal caching probability maximizing the ASE is hard to obtain even numerically. In the

⁴Since when the rate requirement is high, e.g., larger than the backhaul capacity of each PBS, the success probability is zero when the user associates with the PBS tier, we did not compare the success probability of traditional HetNets equipped limited-capacity backhaul with cache-enabled HetNets for conciseness.

following, we first obtain a closed-form expression of an approximated ASE in a special case when the association bias factors are equal, and then try to find the optimal caching probability.

Corollary 4: When $B_1 = B_2$, the ASE of the cache-enabled HetNet can be approximated as

$$\text{ASE} \approx \sum_{k=1}^2 p_{a,k} \lambda_k M_k \left(\ln 2 + \sum_{f=1}^{N_f} \frac{p_f q_{f,k}}{\mathcal{P}_k} \cdot \frac{\alpha}{2\mathcal{K}_{2,fk}} \ln \left(1 + \frac{\mathcal{K}_{2,fk}}{\mathcal{K}_{1,k}} 4^{-\frac{1}{\alpha}} \right) \right) \quad (19)$$

where $\mathcal{K}_{1,k} \triangleq \sum_{j=1}^2 \lambda_{jk} P_{jk}^{\frac{2}{\alpha}} p_{a,j} \Gamma(1 - \frac{2}{\alpha}) \Gamma(M_j + \frac{2}{\alpha}) \Gamma(M_j)^{-1} M_{jk}^{-\frac{2}{\alpha}}$, $\mathcal{K}_{2,fk} \triangleq \sum_{j=1}^2 \lambda_{jk} P_{jk}^{\frac{2}{\alpha}} (1 - p_{a,j})$, and the approximation is accurate when N_c is large and λ_u/λ_2 is small.⁵

Proof: See Appendix G. ■

Although the approximated ASE is in closed-form, the complex expression of \mathcal{P}_k and $p_{a,2}$ with respect to \mathbf{q}_2 makes the optimization problem not concave in general. Only a local optimal solution can be found, e.g., by interior point method [20].

To obtain a closed-form expression for the caching probability, we consider an extreme case.

Corollary 5: When $\lambda_u/\lambda_2 \rightarrow \infty$ and $\lambda_2/\lambda_1 \rightarrow \infty$, the optimal caching probability maximizing the approximated ASE is $q_{1,2}^*, \dots, q_{N_c,2}^* = 1$ and $q_{N_c+1,2}^*, \dots, q_{N_f,2}^* = 0$.

Proof: See Appendix H. ■

Corollary 5 suggests that when the ratios of user-to-helper density and helper-to-MBS density are high, the optimal caching policy maximizing the ASE is to cache the most popular files everywhere, which is quite different from the caching policy maximizing the success probability. The reasons are explained as follows. Although increasing file diversity among helpers can increase the probability of user associated with the helper tier, it may make the user not able to associate with the closest helper, which decreases the signal power and increases the interference power and hence reduces the throughput of each helper. As a consequence, when the user-to-helper density and helper-to-MBS density are high so that all the helper node are active (i.e., each helper has at least one cache-hit user to serve) and the throughput of the helper tier dominates the overall ASE, increasing file diversity leads to low throughput of helper tier and hence low ASE. Therefore, in this case, caching the most popular files everywhere is the ASE-maximal caching policy.

Intuitively, when the user-to-helper density is low such that some helper nodes may have no user to serve, increasing the file diversity among helpers can increase the probability of user

⁵In section V, we show that the approximation is also accurate when N_c is small and λ_u/λ_2 is large by simulation.

associated with the helper tier and hence may increase the active probability of helper. Then, the throughput of each active helper may reduce due to the stronger interference. Nevertheless, we will show in section V that even when the user-to-helper density is low, caching the most popular files everywhere can still achieve near-optimal ASE, because the overall ASE increases with more active helpers.

B. Traditional HetNets

For comparison, we derive the ASE of the traditional HetNet where a tier of MBSs is overlaid with a tier of PBSs with limited capacity backhaul. For notational simplicity, we continue to use λ_2 and P_2 as the density and transmit power of PBS in this subsection. In traditional HetNets, we consider user association based on maximal BRP. Since each MBS and PBS has backhaul and can retrieve all the files from the content server, the traditional HetNet can be regarded as a special case of cache-enabled HetNet when $\mathbf{q}_1 = \mathbf{q}_2 = \mathbf{1}$.

The throughput of PBS in traditional HetNets can not exceed the backhaul capacity. Then, the average throughput of the PBS tier can be expressed as

$$\mathbb{E}\{R_2\} = \mathbb{E}[\min\{W \ln(1 + \gamma_k), C_{\text{bh}}\}] \quad (20)$$

where C_{bh} is the backhaul capacity of each PBS, and function $\min\{x, y\} = x$ if $x \leq y$ and $\min\{x, y\} = y$ otherwise.

Similar to deriving (17) and substituting $\mathbf{q}_1 = \mathbf{q}_2 = \mathbf{1}$, we can obtain the ASE of traditional HetNet as follows, where the only difference lies in the derivation of (20).

Proposition 4: The ASE of traditional HetNet is

$$\text{ASE} = \sum_{k=1}^2 p_{a,k} \lambda_k M_k \frac{1}{P_k} \int_0^{\frac{C_{\text{bh},k}}{W}} \left(\sum_{j=1}^2 \lambda_{jk} (P_{jk} B_{jk})^{\frac{2}{\alpha}} (p_{a,j} Z_{1,jk}(e^x - 1) + 1) \right)^{-1} dx \quad (21)$$

where $C_{\text{bh},1} \rightarrow \infty$, $C_{\text{bh},2} = C_{\text{bh}}$, and $Z_{1,jk}(x)$ is defined in Proposition 3.

Proof: See Appendix I. ■

The computation of the ASE of traditional HetNets requires double numerical integration. To reduce the computational complexity, similar to deriving (19), we obtain the closed-form expression of an approximated ASE of traditional HetNet in the following.

Corollary 6: When $B_1 = B_2$ and $\frac{C_{\text{bh}}}{W} \ll \ln 2$, the ASE of traditional HetNet can be approximated as

$$\text{ASE} \approx \lambda_1 M_1 \left(\ln 2 + \frac{1}{\mathcal{P}_1 K_2} \ln \left(1 + \frac{K_2}{K_1} 4^{-\frac{1}{\alpha}} \right) \right) + \lambda_2 p_{a,2} C_{\text{bh}} \quad (22)$$

where $K_1 \triangleq \sum_{j=1}^2 \lambda_{j1} P_{j1}^{\frac{2}{\alpha}} p_{a,j} \Gamma(1 - \frac{2}{\alpha}) \Gamma(M_j + \frac{2}{\alpha}) \Gamma(M_j)^{-1} M_{j1}^{-\frac{2}{\alpha}}$, and $K_2 \triangleq \sum_{j=1}^2 \lambda_{j1} P_{j1}^{\frac{2}{\alpha}} (1 - p_{a,j})$.

Proof: See Appendix J. ■

Considering that the average download speed of current DSL in USA is about 5 Mbps [6], when the wireless transmission bandwidth is $W = 20$ MHz, we have $C_{\text{bh}}/W = 0.25$ bps/Hz = 0.173 nats/Hz $\ll \ln 2$ and hence the approximation is accurate.

V. SIMULATION AND NUMERICAL RESULTS

In this section, we validate previous analysis via simulation, and demonstrate how different factors affect the optimal caching policies, as well as the corresponding success probability and ASE of cache-enabled HetNet via numerical results.

The following caching policies are considered for comparison,

- 1) Legend “*Max p_s (Inter-point)*”: the local optimal solution of Problem 1 found by interior point method.
- 2) Legend “*Max p_s (Lower-bound)*”: the optimal solution that maximizes the lower bound \underline{p}_s in Proposition 2, i.e., $q_{f,2}^*$.
- 3) Legend “*Max ASE*”: the local optimal solution of Problem 3 found by interior point method.
- 4) Legend “*Popular*”: caching the most popular files everywhere, i.e., $q_{1,2}, \dots, q_{N_c,2} = 1$ and $q_{N_c+1,2}, \dots, q_{N_f,2} = 1$. This policy achieves no file diversity.
- 5) Legend “*Uniform*”: each file is cached with equal caching probability, i.e., $q_{f,2} = N_c/N_f$.

This policy achieves the maximal file diversity.

Unless otherwise specified, the following setting is used. We consider a 3 km \times 3 km square area. The MBS, helper, and user densities are $\lambda_1 = 1/(250^2\pi)$ m⁻², $\lambda_2 = 50/(250^2\pi)$ m⁻² and $\lambda_u = 50/(250^2\pi)$ m⁻², respectively. The path-loss exponent is $\alpha = 3.7$ [21]. The transmit power of each MBS (with $M_1 = 4$ antennas) and helper are $P_1 = 46$ dBm and $P_2 = 21$ dBm, respectively [21]. The bias factors for the MBS and helper tiers are $B_1 = 1$ and $B_2 = 10$, respectively. The transmission bandwidth is $W = 20$ MHz and the minimal rate requirement for

each user is $R_0 = 2$ Mbps. The file catalog size is $N_f = 1000$ files and each helper can cache $N_c = 100$ files, i.e., the normalized cache size is $\eta \triangleq \frac{N_c}{N_f} = 10\%$.

A. Success Probability

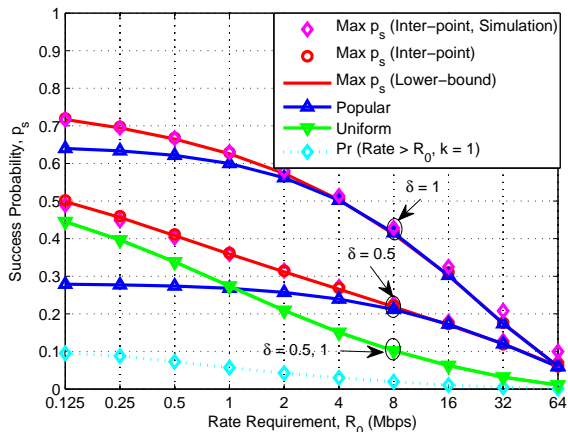


Fig. 2. Validation of the analysis with simulation.

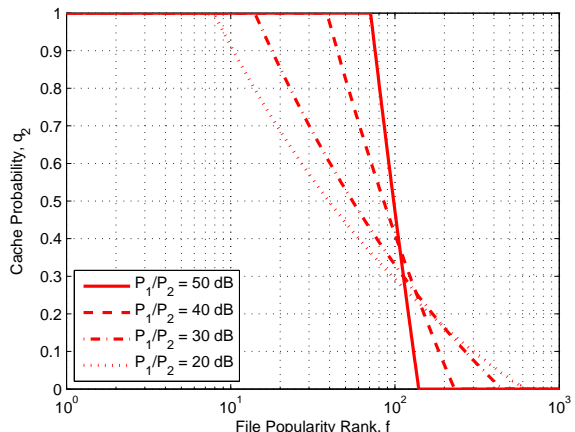


Fig. 3. Impact of difference in transmit powers, $\delta = 0.5$.

In Fig. 2, we show the simulation and numerical results of success probability versus the per-user rate requirement. The simulation result is obtained based on $q_{f,2}^*$ from the interior point method and then by computing $p_s(q_2^*)$ via Monte Carlo method considering -95 dBm noise power. The numerical results are computed from Proposition 1. We can see that the numerical results (with legend “Max p_s (Inter-point)”) is slightly lower than the simulation results (with legend “Max p_s (Inter-point, Simulation)”) when R_0 is low and slightly higher when R_0 is high, because Proposition 1 is derived in interference-limited scenario and by using the approximation on the number of users served by the same helper U_2 in Appendix B. For all the considered caching policies, the simulation results are close to the numerical results, which are not shown for a clean figure. Hence, in the rest of this subsection we only provide the numerical results. We also provide the simulation result of the success probability when the users associate with the MBS tier, i.e. $\mathbb{P}\left(\frac{W}{U_k/M_k} \log_2(1 + \gamma_k) \geq R_0, k = 1\right)$, which is less than 0.05 when $R_0 > 1$ Mbps and hence validates the definition of success probability in (3). Comparing “Max p_s (Lower-bound)” with “Max. p_s (Inter-point)”, we can observe that the caching policy maximizing the lower bound of success probability performs almost the same as the local optimal solution. When the rate requirement is high, e.g., $R_0 > 4$ Mbps for $\delta = 0.5$ or $R_0 > 2$ Mbps for $\delta = 1$, caching the most popular files everywhere can achieve almost the same performance as the optimized

caching policies in this setup with $\lambda_u/\lambda_2 = 1$, which validates Corollary 2 although it is derived when $R_0 \rightarrow \infty$ and $\lambda_u/\lambda_2 \rightarrow \infty$. Moreover, when δ increases, the gap between caching the most popular files everywhere and the optimized caching policies shrinks. These results indicate that for highly skewed demand with high rate requirement, e.g., video on demand service, simply caching the most popular files everywhere can achieve maximal success probability.

In Fig. 3, we show the impact of difference in transmit powers on the optimal caching policy. When P_1/P_2 increases, the files with higher popularity have more chances to be cached while the files with lower popularity have less chances to be cached, which agrees with Corollary 3 although it is derived when $\lambda_u/\lambda_2 \rightarrow 0$. This is because the interference from the MBS increases with P_1/P_2 and caching the most popular file everywhere can increase the user's SINR and hence increase the rate, which leads to the increase of success probability.

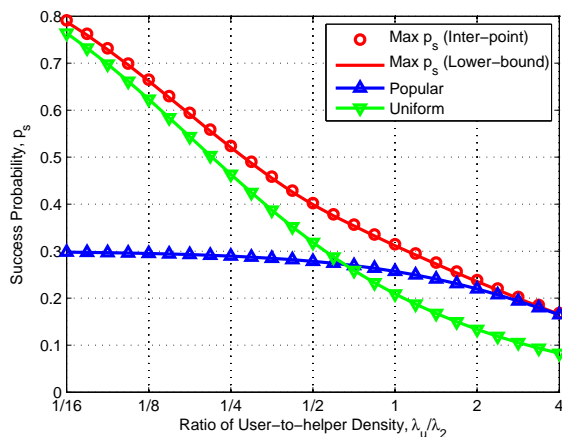


Fig. 4. Impact of helper density, $\delta = 0.5$.

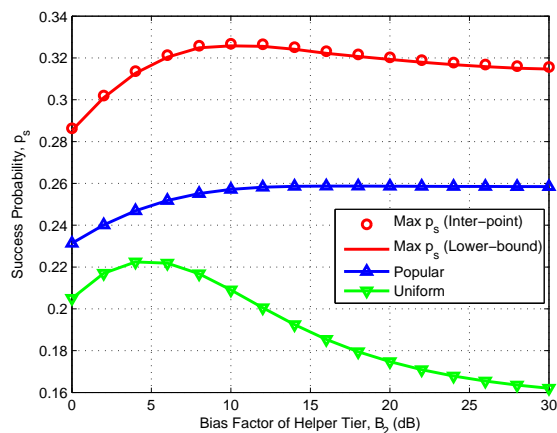


Fig. 5. Impact of bias factor, $B_1 = 1$, $\delta = 0.5$.

In Fig. 4, we show the impact of helper density with given MBS and user densities. We can see that the gain of optimal caching over caching popular files everywhere shrinks when user-to-helper density λ_u/λ_2 increases (λ_1/λ_2 increases as well), which agrees with Corollary 1 and Corollary 3. When λ_u/λ_2 is low, the gain of optimal caching over uniform caching approaches to zero. This can be explained as follows. When λ_2 increases, the SINR at the user associated with the helper tier increases since the helper is closer to the user meanwhile more helpers can be turned into idle mode leading to lower interference. On the other hand, the number of users served by each helper will decrease, hence the time-frequency resources allocated to each user will increase. As a result, the achievable rate of each user will increase and hence the optimal caching probability is less skewed to increase file diversity.

In Fig. 5, we show the impact of the bias factor. We can see that the optimized caching policies outperform the other two policies. When B_2 increases, the success probability first increases and then decreases (though slightly for “Popular”). This is because the users are more likely to associate ASE with the helper tier when B_2 increases, and hence increases the success probability. However, when B_2 continues to increase, the number of users served by each helper also increases, leading to less time-frequency resources allocated to each user. Meanwhile, the distance between the user and its interfering MBS increases since the user prefers a far helper node to associate with than a near MBS, which reduces the SINR of user. Therefore, the success probability finally decreases with B_2 .

B. Area Spectral Efficiency

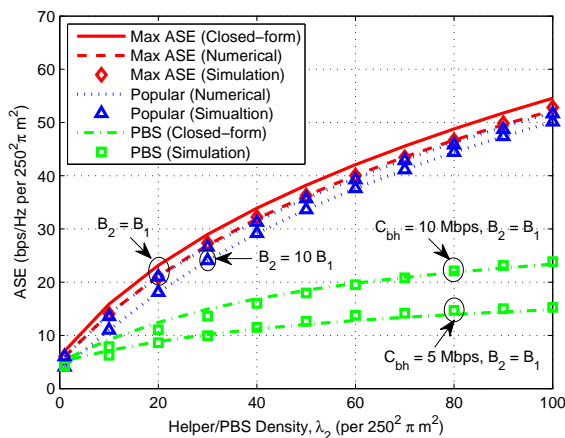


Fig. 6. ASE v.s. helper/PBS density λ_2 , $\delta = 0.5$.

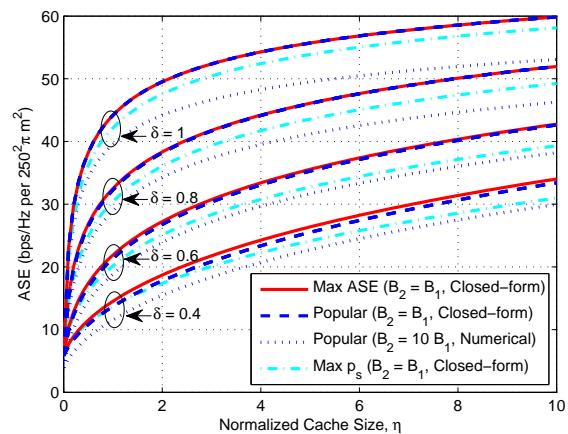


Fig. 7. ASE v.s. normalized cache size η .

In Fig. 6, we show the relation between ASE and helper density and compare the ASE of cache-enabled HetNet with traditional HetNet (with legend “PBS”). The numerical results are obtained from Proposition 3 for cache-enabled HetNet and Proposition 4 for traditional HetNet, the results of the closed-form expression are obtained from Corollary 4 for cache-enabled HetNet and Corollary 6 for traditional HetNet, and the simulation results are obtained by Monte Carlo method considering -95 dBm noise power. We can see that the numerical results derived in interference-limited scenario are almost overlapped with the simulation results for non-biased user association, i.e., $B_2 = B_1$ or biased user association, e.g., $B_2 = 10B_1$. The results obtained from closed-form expressions of approximated ASE are slightly higher than the simulation results when $B_2 = B_1$. The gap is mainly from the approximation in (G.6) where we neglect some small positive terms in the denominator. Nevertheless, the closed-form results are quite accurate and

hence, we only provide the closed-form results in the sequel for conciseness. Moreover, caching the most popular files everywhere can achieve almost the same ASE as the optimal caching policy maximizing the ASE and the gap is minor even when λ_u/λ_2 is small, say $\lambda_u/\lambda_2 = 0.5$ when $\lambda_2 = 100/(250^2\pi)$, which validates Corollary 5 although it is derived when $\lambda_u/\lambda_2 \rightarrow \infty$ and $\lambda_2/\lambda_1 \rightarrow \infty$. Besides, non-bias user association can achieve higher ASE compared with $B_2 = 10B_1$. This is because for biased user association, some users may associate with the helper that offers weaker received signal than a MBS, which reduces the SINR of the users and hence may decrease the ASE.

Compared with the traditional HetNet with limited-capacity backhaul (e.g., $C_{\text{bh}} = 10$ Mbps), the cache-enabled HetNet can double the ASE when each helper node only caches 10% of the total files. Alternatively, to achieve the same ASE, the helper node density is much lower than the PBS density, which can reduce the deployment and operation cost remarkably (e.g., when $C_{\text{bh}} = 10$ Mbps, the helper node density is about 1/3 of the PBS density to achieve an ASE of $20/(250^2\pi)$ bps/Hz/m²).

In Fig. 7, we show the relation between ASE and normalized cache size with different skew parameter δ . As expected, the ASE of cache-enabled HetNet increases with η . Furthermore, when δ is larger, the ASE grows with η more rapidly for small value of η and grows with η more slowly for large η . Moreover, caching the most popular files everywhere can still achieve almost the maximal ASE when η and δ change, especially when δ is large. Besides, by comparing with the results of Fig. 6, we can see that non-biased user association biases can achieve higher ASE than $B_2 = 10B_1$ for different helper density and cache size. Therefore, in the following, we only consider caching the most popular files everywhere with non-biased user association. We also show the ASE based on the caching probability maximizing the success probability when $R_0 = 0.25$ Mbps, which is slight lower than the maximal ASE. By comparing with Fig. 2, we can conclude that when R_0 and δ are high, caching policy maximizing ASE is equivalent to caching maximizing the success probability, while when R_0 and δ are low, the caching policy maximizing ASE suffers a more severe degradation in success probability than the ASE degradation of caching policy maximizing success probability.

Since the ASE of cache-enabled HetNet can be improved either by increasing cache size or helper density, a natural question is: how helper density can be traded off by cache size to achieve a target ASE? To answer this question, we set the ASE as different values and show

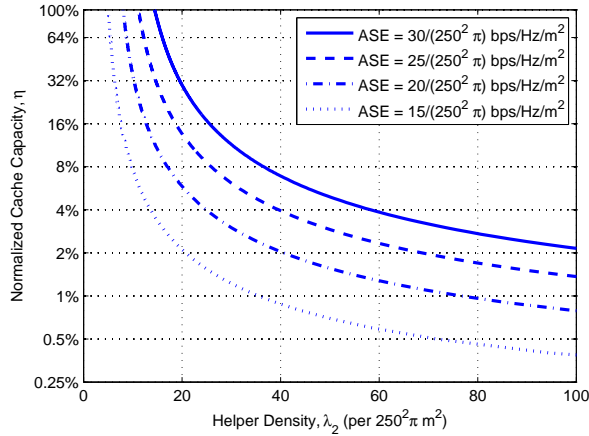


Fig. 8. Trade-off between helper density and cache size, $\delta = 0.5$, $B_2 = B_1$.

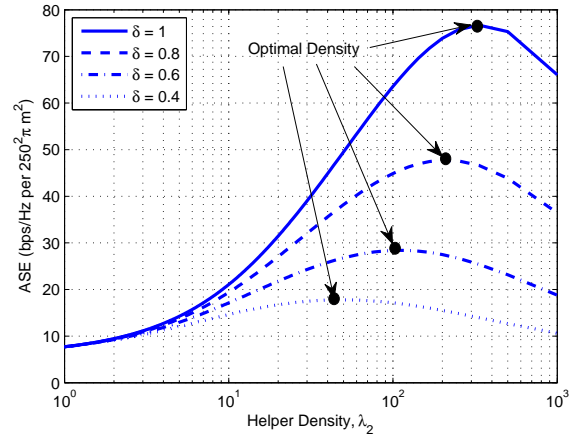


Fig. 9. ASE v.s. helper density with given $\lambda_2 N_c = 10^3/(250^2\pi)$, $B_2 = B_1$.

the normalized cache size versus helper density in Fig. 8. With a given target ASE and cache size N_c , helper density λ_2 can be found from (19) using the bisection search method. We can observe for example that to achieve a target ASE of $20/(250^2\pi)$ bps/Hz/m², by increasing the cache size from $\eta = 1\%$ to $\eta = 2\%$, the helper density can be reduced by half. Similar trade-off between BS density and cache size was reported in [10], where a homogeneous network with single antenna BSs was considered and the performance metric was success probability. When use ASE as the metric, our results show that the helper density can be reduced more significantly by increasing the cache size.

Inspired by such a trade-off, another natural question is: with a given total amount of cache size within an area, should we deploy the caches in a distributed manner (i.e., more helpers each with small cache size) or in a centralized manner (i.e., less helpers each with large cache size) in order to maximize the ASE? To answer this question, we fix the area cache size as a constant, e.g., $\lambda_2 N_c = 10^3/(250^2\pi)$, and provide the ASE versus the helper density in Fig. 9. When $\lambda_2 = 1/(250^2\pi)$, every helper caches all the files, and when $\lambda_2 = 10^3/(250^2\pi)$, each helper caches only one file. We can see that there exists an optimal helper density maximizing the ASE. Moreover, the optimal density increases with δ , which means that the more skewed the file popularity is, the more distributedly we should deploy the caches. This can be explained from the impact of the following two observations in Figs. 6 and 7. On one hand, with given cache size of each helper, the ASE increases with the helper density first rapidly and then slowly. On the other hand, with given helper density, the ASE reduces with the decrease of cache capacity

first slowly and then rapidly, and the larger δ is, the more slowly the ASE decreases with η when the cache size is large.

VI. CONCLUSION

In this paper, we investigated the maximal success probability and ASE of cache-enabled HetNets. Under the probability caching framework, we obtained the optimal caching probability respectively maximizing the success probability and ASE, and analyzed the impact of system settings. Simulation results validated our analysis. The following conclusions can be drawn from the analytical and numerical results. To maximize the success probability, when the MBS-to-helper transmit power ratio, MBS-to-helper density ratio, user-to-helper density ratio or the per-user rate requirement is low, the optimal caching probability is less skewed that achieves file diversity among helpers. Otherwise, caching probability are more skewed. To maximize the ASE, each helper tends to cache the most popular files. Besides, there exists an optimal bias factor to maximize the success probability. By turning the helpers with no user to serve into idle mode, the caching probability should be less skewed to increase file diversity. Compared with traditional HetNet, the helper density is much lower than the PBS density to achieve the same target ASE, and the helper density can be further reduced by increasing cache size. With given total cache size within an area, there exists an optimal helper density that maximizes the ASE.

APPENDIX A: PROOF OF LEMMA 1

Using the law of total probability, we can obtain

$$\mathcal{P}_k = \sum_{f=1}^{N_f} p_k \mathcal{P}_{f,k} \quad (\text{A.1})$$

where $\mathcal{P}_{f,k}$ is the probability of the typical user associated with the k th tier conditioned on that it requests the f th file. Since the user requesting the f th file associates with the BS with the strongest BRP in $\{\Phi_{f,k}\}$ ($k = 1, 2$), which follows independent homogeneous PPP with density $\{q_{f,k}\lambda_k\}$ ($k = 1, 2$) as we mentioned before, $\mathcal{P}_{f,k}$ can be obtained from [9, Lemma 1] as

$$\mathcal{P}_{f,k} = q_{f,k} \left(\sum_{j=1}^2 q_{f,j} \lambda_{jk} (P_{jk} B_{jk})^{\frac{2}{\alpha}} \right)^{-1} \quad (\text{A.2})$$

By substituting (A.2) in to (A.1), Lemma 1 can be proved.

APPENDIX B: PROOF OF PROPOSITION 1

Based on the law of total probability, the success probability can be derived as

$$p_s = \sum_{f=1}^{N_f} p_f \mathbb{P}(\gamma_{f,k} > \gamma_0, k = 2 | f) = \sum_{f=1}^{N_f} p_f \mathcal{P}_{f,2} \mathbb{P}(\gamma_{f,2} > \gamma_0) \quad (\text{B.1})$$

where $\mathbb{P}(\gamma > \gamma_0, k = 2 | f)$ is the success probability conditioned on that the typical user requests the f th file, the last step is from the conditional probability formula and $\mathcal{P}_{f,2}$ can be obtained by (6).

In the following, we derive the general result of $\mathbb{P}(\gamma_{f,k} > \gamma_0)$ and then substitute $k = 2$ to obtain $\mathbb{P}(\gamma_{f,2} > \gamma_0)$. Based on the law of total probability, we have

$$\mathbb{P}(\gamma_{f,k} > \gamma_0) = \int_0^\infty \mathbb{P}(\gamma_{f,k} > \gamma_0 | r) f_{r_k}(r) dr \quad (\text{B.2})$$

where $f_{r_k}(r) = \frac{2\pi q_{f,k} \lambda_k}{\mathcal{P}_{f,k}} r \exp(-\pi r^2 \sum_{j=1}^2 q_{f,j} \lambda_j (P_{jk} B_{jk})^{\frac{2}{\alpha}})$ is the probability density function of the distance between user and its serving BS when requesting the f th file and associated with the k th tier [9], and $\mathbb{P}(\gamma_{f,k} > \gamma_0 | r)$ is the success probability conditioned on that the distance between the typical user and its serving BS is r , which can be derived as,

$$\begin{aligned} \mathbb{P}(\gamma_{f,k} > \gamma_0 | r) &\stackrel{(a)}{=} \mathbb{E}_{U_{f,k}, I_k} [\mathbb{P}(h_{k0} > M_k P_k^{-1} r^\alpha I_k \gamma_0 | r, I_k, U_{f,k})] \\ &\stackrel{(b)}{=} \mathbb{E}_{U_{f,k}, I_k} [\exp(-M_k P_k^{-1} r^\alpha I_k \gamma_0)] \\ &\stackrel{(c)}{=} \mathbb{E}_{U_{f,k}} \left[\prod_{j=1}^2 \mathcal{L}_{I_{f,kj}}(M_k P_k^{-1} r^\alpha \gamma_0) \prod_{j=1}^2 \mathcal{L}_{I_{f',kj}}(M_k P_k^{-1} r^\alpha \gamma_0) \right] \\ &\stackrel{(d)}{=} \sum_{U_{f,k}=n}^\infty \mathbb{P}(U_{f,k} = n) \left(\prod_{j=1}^2 \mathcal{L}_{I_{f,kj}}(M_k P_k^{-1} r^\alpha \gamma_0) \prod_{j=1}^2 \mathcal{L}_{I_{f',kj}}(M_k P_k^{-1} r^\alpha \gamma_0) \right) \Big|_{U_{f,k}=n} \end{aligned} \quad (\text{B.3})$$

where $U_{f,k}$ is the number of users served by the same BS together with the typical user when the typical user requests the f th file and associates with the k th tier, step (a) is from (2) by neglecting the thermal noise, step (b) is from $h_{k0} \sim \exp(1)$, step (c) follows because $\mathcal{L}_{\sum_j I_{f,kj}}(s) = \prod_i \mathcal{L}_{I_{f,kj}}(s)$, and $\mathcal{L}(\cdot)$ denotes the Laplace transform, step (d) is from the law of total probability. The value of γ_0 depends on $U_{f,k}$, which is $\gamma_0 = 2^{\frac{R_0 U_{f,k}}{W M_k}} - 1$.

To derive the Laplace transform of $I_{k,j}$, we model the distribution of the active BSs in j th tier as PPP with density $p_{a,j} \lambda_j$ by thinning the PPP Φ_j with probability $p_{a,j}$ [22], where $p_{a,j}$ is the probability that a randomly chosen BS in the j th tier is active, which can be derived as

$$p_{a,j} = 1 - \int_0^\infty e^{-\lambda_u x} f_{S_j}(x) dx \approx 1 - \left(1 + \frac{P_j \lambda_u}{3.5 \lambda_j}\right)^{-3.5} \quad (\text{B.4})$$

where $f_{S_j}(x)$ is the PDF of the service area S_j of the BS in the k th tier, and the approximation comes from $f_{S_j}(x) \approx \frac{3.5^{3.5}}{\Gamma(3.5)} \left(\frac{\lambda_j}{P_j}\right)^{3.5} x^{2.5} e^{-3.5\lambda_j x/P_j}$ in [23], which is accurate when $\lambda_2 \gg \lambda_1$. For $k = 1$ (i.e., the MBS tier), $p_{a,1}$ exactly equals to 1 since $\lambda_u/\lambda_1 \rightarrow \infty$.

Then, the distribution of the active BSs in the j th tier caching the f th file $\tilde{\Phi}_{f,k}$ and those not caching the f th file $\tilde{\Phi}_{f',j}$ are two homogeneous PPP with density $p_{a,j}q_{f,j}\lambda_j$ and $p_{a,j}(1-q_{f,j})q_{f,j}\lambda_j$. The Laplace transform of $I_{f,kj}$ in (B.3) can be derived as

$$\begin{aligned} \mathcal{L}_{I_{f,kj}}(s) &= \mathbb{E}_{\tilde{\Phi}_{f,j}, h_{ji}} \left[e^{-s \sum_{i \in \tilde{\Phi}_{f,j} \setminus b_{k0}} P_j h_{ji} r_{ji}^{-\alpha_j}} \right] \\ &\stackrel{(a)}{=} \mathbb{E}_{\tilde{\Phi}_{f,j}} \left[\prod_{i \in \tilde{\Phi}_{f,j} \setminus b_{k0}} \left(1 + \frac{s P_j}{M_j} r_{j,i}^{-\alpha_j} \right)^{-M_j} \right] \\ &\stackrel{(b)}{=} e^{-2\pi p_{a,j} q_{f,j} \lambda_j \int_{r_{0j}}^{\infty} \left(1 - \left(1 + \frac{s P_j}{M_j} v^{-\alpha_j} \right)^{-M_j} \right) v dv} \\ &= e^{-\pi p_{a,j} q_{f,j} \lambda_j r_{0j}^2 \left(F_1 \left[-\frac{2}{\alpha}, M_j; 1 - \frac{2}{\alpha}; -\frac{s P_j}{M_j} r_{0j}^{-\alpha} \right] - 1 \right)} \end{aligned} \quad (\text{B.5})$$

where step (a) follows from $h_{ji} \sim \mathbb{G}(M_j, 1/M_j)$, step (b) follows from the probability generating function of the PPP, and $r_{0j} = (P_{jk} B_{jk})^{\frac{1}{\alpha}} r$ is the closest possible distance of the interfering BS in $\tilde{\Phi}_{f,j}$. Substituting r_{0j} and $s = M_k P_k^{-1} r^\alpha \gamma_0$ into (B.5), we obtain

$$\mathcal{L}_{f,kj}(M_k P_k^{-1} r^\alpha \gamma_0) = e^{-\pi p_{a,j} q_{f,j} \lambda_j (P_{jk} B_{jk})^{\frac{2}{\alpha}} r^2 Z_{1,kj}(\gamma_0)} \quad (\text{B.6})$$

where $Z_{1,kj}(\gamma_0) \triangleq {}_2F_1 \left[-\frac{2}{\alpha}, M_j; 1 - \frac{2}{\alpha}; -\frac{\gamma_0}{M_{jk} B_{jk}} \right] - 1$.

Since the BSs not caching the f th file, i.e. $\tilde{\Phi}_{f',j}$, can be arbitrarily close to the user, i.e., $r_{0j} \rightarrow 0$, from $\lim_{r_{0j} \rightarrow 0} r_{0j}^2 ({}_2F_1 \left[-\frac{2}{\alpha}, M_j; 1 - \frac{2}{\alpha}; -\frac{s P_j}{M_j} r_{0j}^{-\alpha} \right] - 1) = \Gamma(1 - \frac{2}{\alpha}) \Gamma(M_j + \frac{2}{\alpha}) \Gamma(M_j)^{-1} (\frac{s P_j}{M_j})^{\frac{2}{\alpha}}$, similar to the derivation of (B.5), we can obtain

$$\mathcal{L}_{f',kj}(M_k P_k^{-1} r^\alpha \gamma_0) = e^{-\pi p_{a,j} (1-q_{f,j}) \lambda_j P_{jk}^{\frac{2}{\alpha}} r^2 Z_{2,kj}(\gamma_0)} \quad (\text{B.7})$$

where $Z_{2,kj}(\gamma_0) \triangleq \Gamma(1 - \frac{2}{\alpha}) \Gamma(M_j + \frac{2}{\alpha}) \Gamma(M_j)^{-1} (\frac{\gamma_0}{M_{jk}})^{\frac{2}{\alpha}}$.

By substituting (B.6) and (B.7) into (B.3), further considering (B.2) and $\int_0^\infty 2r e^{-Ar^2} dr = \frac{1}{A}$, we obtain

$$\begin{aligned} \mathbb{P}(\gamma_{f,k} > \gamma_0) &= \sum_{n=1}^{\infty} \mathbb{P}(U_{f,k} = n) \frac{q_{f,k}}{\mathcal{P}_{f,k}} \left(\sum_{j=1}^2 \lambda_{jk} P_{jk}^{\frac{2}{\alpha}} \left(q_{f,j} p_{a,j} B_{jk}^{\frac{2}{\alpha}} Z_{1,jk}(\gamma_0) \right. \right. \\ &\quad \left. \left. + (1 - q_{f,j}) p_{a,j} Z_{2,jk}(\gamma_0) + q_{f,j} B_{jk}^{\frac{2}{\alpha}} \right) \right)^{-1} \Bigg|_{U_{f,k}=n} \end{aligned} \quad (\text{B.8})$$

where $\mathbb{P}(U_{f,k} = n)$ can be obtained from the tier association probability $\mathcal{P}_{f,k}$ based on [23, Lemma 3], which however has a very complicated expression. To simplify the analysis, we approximate $U_{f,k}$ by the average number of users served by the same BS in the k th tier from [23, Corollary 1], i.e., $U_{f,k} \approx \mathbb{E}[U_k] = 1 + \frac{1.28\lambda_u \mathcal{P}_k}{\lambda_k}$, which is verified to have negligible impact on the success probability by simulation in section V. Specially, when $\lambda_u/\lambda_k \rightarrow 0$, i.e., the user density is low such that each helper serves at most one user, then $U_{f,k} = \mathbb{E}[U_k] = 1$, and the approximation becomes exact. Upon using the approximation, (B.8) becomes

$$\mathbb{P}(\gamma_{f,k} > \gamma_0) = \frac{q_{f,k}}{\mathcal{P}_{f,k}} \left(\sum_{j=1}^2 \lambda_{jk} P_{jk}^{\frac{2}{\alpha}} \left(q_{f,j} p_{a,j} B_{jk}^{\frac{2}{\alpha}} Z_{1,jk}(\gamma_0) + (1 - q_{f,j}) p_{a,j} Z_{2,jk}(\gamma_0) + q_{f,j} B_{jk}^{\frac{2}{\alpha}} \right) \right)^{-1} \quad (\text{B.9})$$

where $\gamma_0 \triangleq 2^{\frac{R_0 U_{f,k}}{WM_k}} - 1 \approx 2^{\frac{R_0 \mathbb{E}[U_k]}{WM_k}} - 1 = 2^{\frac{R_0}{WM_k} \left(1 + \frac{1.28\lambda_u \mathcal{P}_k}{\lambda_k}\right)} - 1$.

Then, by substituting $k = 2$, $q_{f,1} = 1$, $M_2 = 1$ and $p_{a,1} = 1$ into (B.9) and then into (B.1), Proposition 1 can be proved.

APPENDIX C: PROOF OF COROLLARY 1

Without loss of generality, we assume $\underline{q}_{1,2}^*, \dots, \underline{q}_{N_1,2}^* = 1$ and $\underline{q}_{N_f - N_0 + 1,2}^*, \dots, \underline{q}_{N_f,2}^* = 0$. By defining $c_1 \triangleq C_{1,\bar{\gamma}_0} + \bar{p}_{a,2} C_{2,\bar{\gamma}_0}$ and $c_2 \triangleq \bar{p}_{a,2} C_{3,\bar{\gamma}_0} + 1$, from $\sum_{f=1}^{N_f} \underline{q}_{f,2}^* = N_c$ and (12), we have $\sum_{f=N_0+1}^{N_f - N_1} \left(\frac{1}{c_2} \sqrt{\frac{c_1}{\nu}} \sqrt{p_f} - \frac{c_1}{c_2} \right) + N_1 = N_c$, from which we obtain

$$\frac{1}{c_2} \sqrt{\frac{c_1}{\nu}} = \frac{N_c - N_1 + (N_f - N_0 - N_1) \frac{c_1}{c_2}}{\sum_{f=N_0+1}^{N_f - N_1} \sqrt{p_f}} \quad (\text{C.1})$$

As shown in (C.1), $\frac{1}{c_2} \sqrt{\frac{c_1}{\nu}}$ increases with c_1/c_2 . Since $C_{2,\bar{\gamma}_0} \geq 0$ and $C_{3,\bar{\gamma}_0} \leq 0$, c_1/c_2 increases with $\bar{p}_{a,2}$ and hence $\frac{1}{c_2} \sqrt{\frac{c_1}{\nu}}$ increases with $\bar{p}_{a,2}$. Further considering that $p_{a,2}$ increases with λ_u/λ_2 , we know that $\frac{1}{c_2} \sqrt{\frac{c_1}{\nu}}$ increases with λ_u/λ_2 .

For any $\underline{q}_{f,2}^*, \underline{q}_{f+1,2}^* \in (0, 1)$, from (12), we have

$$\underline{q}_{f,2}^* - \underline{q}_{f+1,2}^* = \frac{1}{c_2} \sqrt{\frac{c_1}{\nu}} (p_f - p_{f+1}) \quad (\text{C.2})$$

Since $p_f > p_{f+1}$, $\underline{q}_{f,2}^* - \underline{q}_{f+1,2}^*$ increases with $\frac{1}{c_2} \sqrt{\frac{c_1}{\nu}}$ and hence increases with λ_u/λ_2 .

APPENDIX D: PROOF OF COROLLARY 2

Since $R_0 \rightarrow \infty$ is equivalent to $\bar{\gamma}_0 \rightarrow \infty$, in the following we analyze the case for $\bar{\gamma}_0 \rightarrow \infty$ instead. By employing the transformation of ${}_2F_1[a, b; c; z]$ from [24, eq. (9.132)]

$$\begin{aligned}
{}_2F_1[a, b; c; z] &= \frac{\Gamma(c)\Gamma(b-a)}{\Gamma(b)\Gamma(c-a)} (-z)^{-a} {}_2F_1\left[a, a+1-c; a+1-b; \frac{1}{z}\right] \\
&\quad + \frac{\Gamma(c)\Gamma(a-b)}{\Gamma(a)\Gamma(c-b)} (-z)^{-b} {}_2F_1\left[b, b+1-c; b+1-a; \frac{1}{z}\right] \quad (\text{D.1})
\end{aligned}$$

and considering the series-form expression of ${}_2F_1[a, b; c; z] = \sum_{n=0}^{\infty} \frac{(a)_n(b)_n}{(c)_n} z^n$ where $(x)_n \triangleq x(x+1)\cdots(x+n-1)$ denotes the rising Pochhammer symbol, we can obtain the asymptotic result of ${}_2F_1\left[-\frac{2}{\alpha}, M_2; 1-\frac{2}{\alpha}; -\bar{\gamma}_0\right]$ for $\bar{\gamma}_0 \rightarrow \infty$ as,

$${}_2F_1\left[-\frac{2}{\alpha}, M_2; 1-\frac{2}{\alpha}; -\bar{\gamma}_0\right] = \frac{\Gamma(1-\frac{2}{\alpha})\Gamma(M_2+\frac{2}{\alpha})}{\Gamma(M_2)} \bar{\gamma}_0^{\frac{2}{\alpha}} + \mathcal{O}(\bar{\gamma}_0^{-M_2}) \quad (\text{D.2})$$

which equals $C_{2, \bar{\gamma}_0}$ when $\bar{\gamma}_0 \rightarrow \infty$. Then, considering the definition of $C_{3, \bar{\gamma}_0}$, we have $\lim_{\bar{\gamma}_0 \rightarrow \infty} C_{3, \bar{\gamma}_0} = \lim_{\bar{\gamma}_0 \rightarrow \infty} {}_2F_1\left[-\frac{2}{\alpha}, M_2; 1-\frac{2}{\alpha}; -\bar{\gamma}_0\right] - C_{2, \bar{\gamma}_0} - 1 = -1$. Upon substituting $C_{3, \bar{\gamma}_0} = -1$ into (13), we obtain $\lim_{R_0 \rightarrow \infty} p_s(\mathbf{q}_2) = \lim_{\bar{\gamma}_0 \rightarrow \infty} p_s(\mathbf{q}_2) = \frac{1}{C_{1, \bar{\gamma}_0}} \sum_{f=1}^{N_f} p_f q_{f,2}$. Since p_f decreases with f and further considering constraint (8a) and (8b), it is easy to see that the optimal values of $q_{f,2}$ maximizing $\sum_{f=1}^{N_f} p_f q_{f,2}$ are $q_{1,2}^*, \dots, q_{N_c,2}^* = 1$ and $q_{N_c+1,2}^*, \dots, q_{N_f,2}^* = 0$, and hence Corollary 2 is proved.

APPENDIX E: PROOF OF COROLLARY 3

Without loss of generality, we assume $q_{1,2}^*, \dots, q_{N_1,2}^* = 1$ and $q_{N_f-N_0+1,2}^*, \dots, q_{N_f,2}^* = 0$, from $\sum_{f=1}^{N_f} q_{f,2}^* = N_c$ and (16), similar to the derivation of (C.1), we can obtain

$$\sqrt{\frac{C_{1, \gamma_0}}{\nu}} = \frac{N_c - N_1 + (N_f - N_0 - N_1)C_{1, \gamma_0}}{\sum_{f=N_0+1}^{N_f-N_1} \sqrt{p_f}} \quad (\text{E.1})$$

As shown in (E.1), $\sqrt{\frac{C_{1, \gamma_0}}{\nu}}$ increases with C_{1, γ_0} . Considering that C_{1, γ_0} increases with λ_{12} and P_{12} , $\sqrt{\frac{C_{1, \gamma_0}}{\nu}}$ increases with λ_{12} and P_{12} .

Then, similar to (C.2), for any $q_{f,2}^*, q_{f+1,2}^* \in (0, 1)$, we have

$$q_{f,2}^* - q_{f+1,2}^* = \sqrt{\frac{C_{1, \gamma_0}}{\nu}} (p_f - p_{f+1}) \quad (\text{E.2})$$

and $q_{f,2}^* - q_{f+1,2}^*$ increases with $\sqrt{\frac{C_{1, \gamma_0}}{\nu}}$ and hence increases with λ_{12} and P_{12} .

APPENDIX F: PROOF OF PROPOSITION 3

Denoting γ_{uk} as the SINR of the u th user served by the BS in the k th tier, the average throughput of an active BS in the k th tier can be expressed as

$$\mathbb{E}[R_k] = \mathbb{E}\left[\sum_{u=1}^{U_k} \frac{W}{U_k/M_k} \ln(1 + \gamma_{uk})\right] = W M_k \mathbb{E}[\ln(1 + \gamma_{uk})] \quad (\text{F.1})$$

where the last step follows because γ_{uk} ($u = 1, \dots, U_k$) are independently and identically distributed. By taking the expectation over the random file request, we have

$$\mathbb{E}[\ln(1 + \gamma_{uk})] = \sum_{f=1}^{N_f} p_{f,k} \mathbb{E}[\ln(1 + \gamma_{f,k})] \quad (\text{F.2})$$

where $p_{f,k} = \frac{p_f \mathcal{P}_{f,k}}{\mathcal{P}_k}$ obtained from conditional probability formula is the probability that the u th user served by the BS in the k th tier requests the f th file. Since $\mathbb{E}[X] = \int_0^\infty \mathbb{P}(X > x) dx$ for $X > 0$, $\mathbb{E}[\ln(1 + \gamma_{k,f})]$ can be derived as

$$\mathbb{E}[\ln(1 + \gamma_{f,k})] = \int_0^\infty \mathbb{P}(\ln(1 + \gamma_{f,k}) > x) dx = \int_0^\infty \mathbb{P}(\gamma_{f,k} > e^x - 1) dx \quad (\text{F.3})$$

Similar to deriving (B.8), we can obtain

$$\begin{aligned} \mathbb{P}(\gamma_{f,k} > e^x - 1) = \frac{q_{f,k}}{\mathcal{P}_{f,k}} \left(\sum_{j=1}^2 \lambda_{jk} P_{jk}^{\frac{2}{\alpha}} \left(q_{f,j} p_{a,j} B_{jk}^{\frac{2}{\alpha}} Z_{1,jk}(e^x - 1) \right. \right. \\ \left. \left. + (1 - q_{f,j}) p_{a,j} Z_{2,jk}(e^x - 1) + q_{f,j} B_{jk}^{\frac{2}{\alpha}} \right) \right)^{-1} \quad (\text{F.4}) \end{aligned}$$

Upon substituting (F.4) into (F.3) and furthering considering (F.2), (F.1) and (4), Proposition 3 can be proved.

APPENDIX G: PROOF OF COROLLARY 4

To obtain a closed-form approximation for the integration in (17) (denoted as $\text{Int}_{fk}(x)|_0^\infty$ in the following). We first derive the asymptotic results of $Z_{1,jk}(e^x - 1)$ and $Z_{2,jk}(e^x - 1)$ for $x \rightarrow 0$ and $x \rightarrow \infty$, respectively. We consider $B_1 = B_2$, i.e., $B_{jk} = 1$, in the following derivations.

From the series-form expression of ${}_2F_1[a, b; c; z] = \sum_{n=0}^\infty \frac{(a)_n (b)_n}{(c)_n} z^n$, we have the asymptotic expression of ${}_2F_1[a, b; c; z]$ for $x \rightarrow 0$ as ${}_2F_1[a, b; c; z] = 1 + \mathcal{O}(x)$. Then, the asymptotic expression of $Z_{1,jk}(e^x - 1)$ for $x \rightarrow 0$ can be expressed as

$$Z_{1,jk}(e^x - 1) = {}_2F_1 \left[-\frac{2}{\alpha}, M_j; 1 - \frac{2}{\alpha}; -\frac{e^x - 1}{M_{jk} B_{jk}} \right] - 1 = 1 + \mathcal{O}(1 - e^x) - 1 \stackrel{(a)}{=} x + \mathcal{O}(x^2) \quad (\text{G.1})$$

where step (a) is from $1 - e^x = x + \mathcal{O}(x^2)$ and the approximation is accurate for $1 - e^x \ll 1$, i.e., $x \ll \ln 2$. In this case, the asymptotic expression of $Z_{2,jk}(e^x - 1)$ for $x \rightarrow 0$ can be expressed as

$$Z_{2,jk}(e^x - 1) = \frac{\Gamma(1 - \frac{2}{\alpha}) \Gamma(M_j + \frac{2}{\alpha})}{\Gamma(M_j)} \left(\frac{e^x - 1}{M_{jk}} \right)^{\frac{2}{\alpha}} = \frac{\Gamma(1 - \frac{2}{\alpha}) \Gamma(M_j + \frac{2}{\alpha})}{\Gamma(M_j) M_{jk}^{\frac{2}{\alpha}}} x^{\frac{2}{\alpha}} + \mathcal{O}(x^{\frac{4}{\alpha}}) \quad (\text{G.2})$$

When $x \rightarrow \infty$, similar to the derivation of (D.2), we can obtain the asymptotic results of $Z_{1,fk}(e^x - 1)$ for $x \rightarrow \infty$ as,

$$\begin{aligned} Z_{1,jk}(e^x - 1) &= \frac{\Gamma(1-\frac{2}{\alpha})\Gamma(M_j+\frac{2}{\alpha})}{\Gamma(M_j)M_{jk}^{\frac{2}{\alpha}}} (e^x - 1)^{\frac{2}{\alpha}} - 1 + \mathcal{O}((e^x - 1)^{-M_j}) \\ &\approx \frac{\Gamma(1-\frac{2}{\alpha})\Gamma(M_j+\frac{2}{\alpha})}{\Gamma(M_j)M_{jk}^{\frac{2}{\alpha}}} e^{\frac{2x}{\alpha}} - 1 \end{aligned} \quad (\text{G.3})$$

where the last step is from omits “1” for $e^x - 1$ and the approximation is accurate when $e^x - 1 \gg 1$, i.e., $x \gg \ln 2$. Then, the asymptotic expression of $Z_{2,jk}(e^x - 1)$ for $x \rightarrow \infty$ can be expressed as

$$Z_{2,jk}(e^x - 1) \approx \frac{\Gamma(1-\frac{2}{\alpha})\Gamma(M_j+\frac{2}{\alpha})}{\Gamma(M_j)M_{jk}^{\frac{2}{\alpha}}} e^{\frac{2x}{\alpha}} \quad (\text{G.4})$$

By dividing the integration limits from $[0, \infty)$ to $[0, \ln 2]$ and $[\ln 2, \infty)$, we have

$$\text{Int}_{fk}(x)|_0^\infty = \text{Int}_{fk}(x)|_0^{\ln 2} + \text{Int}_{fk}(x)|_{\ln 2}^\infty \quad (\text{G.5})$$

Employing the approximation in (G.1) and (G.2) for $Z_{1,jk}(e^x - 1)$ and $Z_{2,jk}(e^x - 1)$ when $x \in [0, \ln 2]$, we can approximate $\text{Int}_{fk}(x)|_0^{\ln 2}$ as

$$\begin{aligned} \text{Int}_{fk}(x)|_0^{\ln 2} &\approx \int_0^{\ln 2} \left(\sum_{j=1}^2 \lambda_{jk} P_{jk}^{\frac{2}{\alpha}} \left(q_{f,j} p_{a,j} x + (1 - q_{f,j}) p_{a,j} \frac{\Gamma(1-\frac{2}{\alpha})\Gamma(M_j+\frac{2}{\alpha})}{\Gamma(M_j)M_{jk}^{\frac{2}{\alpha}}} x^{\frac{2}{\alpha}} + q_{f,j} \right) \right)^{-1} dx \\ &\approx \int_0^{\ln 2} \left(\sum_{j=1}^2 \lambda_{jk} P_{jk}^{\frac{2}{\alpha}} q_{f,j} \right)^{-1} dx = \left(\sum_{j=1}^2 q_{f,j} \lambda_{jk} P_{jk}^{\frac{2}{\alpha}} \right)^{-1} \ln 2 \end{aligned} \quad (\text{G.6})$$

The last approximation is accurate when $q_{f,j} p_{a,j} x + (1 - q_{f,j}) p_{a,j} \frac{\Gamma(1-\frac{2}{\alpha})\Gamma(M_j+\frac{2}{\alpha})}{\Gamma(M_j)M_{jk}^{\frac{2}{\alpha}}} x^{\frac{2}{\alpha}} \Big|_{x=\ln 2} \ll q_{f,j}$. For the MBS tier, $q_1 = 1$, we have $q_{f,1} p_{a,1} x + (1 - q_{f,1}) p_{a,1} \frac{\Gamma(1-\frac{2}{\alpha})\Gamma(M_1+\frac{2}{\alpha})}{\Gamma(M_1)M_{1k}^{\frac{2}{\alpha}}} x^{\frac{2}{\alpha}} \Big|_{x=\ln 2} = \ln 2 < 1$ and for the helper tier, the condition holds when $q_{f,2}$ is large and $p_{a,2}$ is small. Since the cache probability $q_{f,2}$ increases with cache size N_c and $p_{a,2}$ increases with λ_u/λ_2 as shown in Proposition 1, the approximation is accurate when N_c is large and λ_u/λ_2 is small. In section V, we show that the approximation is also accurate when N_c is small and λ_u/λ_2 is large by simulation.

Employing the approximation in (G.3) and (G.4) for $Z_{1,jk}(e^x - 1)$ and $Z_{2,jk}(e^x - 1)$ when $x \in [\ln 2, \infty)$, we obtain

$$\begin{aligned} \text{Int}_{fk}(x)|_{\ln 2}^\infty &\approx \int_{\ln 2}^\infty \left(\sum_{j=1}^2 \lambda_{jk} P_{jk}^{\frac{2}{\alpha}} p_{a,j} \frac{\Gamma(1-\frac{2}{\alpha})\Gamma(M_j+\frac{2}{\alpha})}{\Gamma(M_j)M_{jk}^{\frac{2}{\alpha}}} e^{\frac{2x}{\alpha}} + \sum_{j=1}^2 \lambda_{jk} P_{jk}^{\frac{2}{\alpha}} q_{f,j} (1 - p_{a,j}) \right)^{-1} dx \\ &= \frac{\alpha}{2K_{2,fk}} \ln \left(1 + \frac{K_{2,fk}}{K_{1,k}} 4^{-\frac{1}{\alpha}} \right) \end{aligned} \quad (\text{G.7})$$

where $K_{1,k} \triangleq \sum_{j=1}^2 \lambda_{jk} P_{jk}^{\frac{2}{\alpha}} p_{a,j} \Gamma(1 - \frac{2}{\alpha}) \Gamma(M_j + \frac{2}{\alpha}) \Gamma(M_j)^{-1} M_{jk}^{-\frac{2}{\alpha}}$, and $K_{2,fk} \triangleq \sum_{j=1}^2 \lambda_{jk} P_{jk}^{\frac{2}{\alpha}} q_{f,j} (1 - p_{a,j})$.

Upon substituting (G.6) and (G.7) into (G.5) and further considering (17), we have

$$\begin{aligned} \text{ASE} &\approx \sum_{k=1}^2 p_{a,k} \lambda_k M_k \sum_{f=1}^{N_f} \frac{p_f q_{f,k}}{\mathcal{P}_k} \left(\frac{\ln 2}{\sum_{j=1}^2 q_{f,j} \lambda_{jk} P_{jk}^{\frac{2}{\alpha}}} + \frac{\alpha}{2K_{2,fk}} \ln \left(1 + \frac{K_{2,fk}}{K_{1,k}} 4^{-\frac{1}{\alpha}} \right) \right) \\ &= \sum_{k=1}^2 p_{a,k} \lambda_k M_k \left(\ln 2 + \sum_{f=1}^{N_f} \frac{p_f q_{f,k}}{\mathcal{P}_k} \cdot \frac{\alpha}{2K_{2,fk}} \ln \left(1 + \frac{K_{2,fk}}{K_{1,k}} 4^{-\frac{1}{\alpha}} \right) \right) \end{aligned} \quad (\text{G.8})$$

where the last equation is from $\mathcal{P}_k = \sum_{f=1}^{N_f} (p_f q_{f,k} / \sum_{j=1}^2 q_{f,j} \lambda_{jk} P_{jk}^{\frac{2}{\alpha}})$ given by Lemma 1.

APPENDIX H: PROOF OF COROLLARY 5

With $\lambda_u / \lambda_2 \rightarrow \infty$, we have $p_{a,k} \rightarrow 1$ and $K_{2,fk} \rightarrow 0$. Then, (19) degenerates into,

$$\text{ASE} \approx \sum_{k=1}^2 \lambda_k M_k \left(\ln 2 + \frac{\alpha}{2K_{1,k} \mathcal{P}_k} 4^{-\frac{1}{\alpha}} \sum_{f=1}^{N_f} p_f q_{f,k} \right) \quad (\text{H.1})$$

Further considering $\lambda_2 / \lambda_1 \rightarrow \infty$, we have $\mathcal{P}_2 \rightarrow 1$ and

$$\text{ASE} \approx \lambda_2 M_2 \left(\ln 2 + \frac{\alpha}{2K_{1,2}} 4^{-\frac{1}{\alpha}} \sum_{f=1}^{N_f} p_f q_{f,2} \right) \quad (\text{H.2})$$

Since $K_{1,k}$ does not depend on $q_{f,k}$, from (H.2) we can see that maximizing ASE is equivalent to maximizing $\sum_{f=1}^{N_f} p_f q_{f,2}$. Further considering constraints (8a) and (8b), we can easily obtain the optimal caching probability as $q_{1,2}^*, \dots, q_{N_c,2}^* = 1$ and $q_{N_c+1,2}^*, \dots, q_{N_f,2}^* = 0$.

APPENDIX I: PROOF OF PROPOSITION 4

For the PBS tier, based on the law of total probability, from (20) we obtain

$$\begin{aligned} \mathbb{E}[R_2] &= \sum_{f=1}^{N_f} p_{f,2} \mathbb{E}[\min\{W \ln(1 + \gamma_{f,2}), C_{\text{bh}}\}] = W \sum_{f=1}^{N_f} p_{f,2} \mathbb{E}[\min\{\ln(1 + \gamma_{f,2}), \frac{C_{\text{bh}}}{W}\}] \\ &= W \sum_{f=1}^{N_f} p_{f,2} \int_0^\infty \mathbb{P}[\min\{\ln(1 + \gamma_{f,2}), \frac{C_{\text{bh}}}{W}\} > x] dx \\ &= W \sum_{f=1}^{N_f} p_{f,2} \int_0^{\frac{C_{\text{bh}}}{W}} \mathbb{P}[\log_2(1 + \gamma_{f,2}) > x] dx \end{aligned} \quad (\text{I.1})$$

where the last step is from $\mathbb{P}[\min\{\log_2(1 + \gamma_{f,2}), \frac{C_{\text{bh}}}{W}\} > x] = 0$ for $x > \frac{C_{\text{bh}}}{W}$ and $\mathbb{P}[\min\{\log_2(1 + \gamma_{f,2}), \frac{C_{\text{bh}}}{W}\} > x] = \mathbb{P}[\log_2(1 + \gamma_{f,2}) > x]$ for $0 \leq x \leq \frac{C_{\text{bh}}}{W}$.

Since the traditional HetNet can be regarded as a special case of cache-enabled HetNets when $\mathbf{q}_1 = \mathbf{q}_2 = \mathbf{1}$, by substituting (F.4) with $k = 2$ and $\mathbf{q}_1 = \mathbf{q}_2 = \mathbf{1}$ into (I.1), we have

$$\mathbb{E}[R_2] = \frac{W}{\mathcal{P}_2} \int_0^{\frac{C_{\text{bh}}}{W}} \left(\sum_{j=1}^2 \lambda_{j2} (P_{j2} B_{j2})^{\frac{2}{\alpha}} (p_{a,j} Z_{1,j2}(e^x - 1) + 1) \right)^{-1} dx \quad (\text{I.2})$$

where $p_{a,1} = 1$ and $p_{a,2} \approx 1 - \left(1 + \frac{P_j \lambda_u}{3.5 \lambda_j}\right)^{-3.5}$.

Since the deployment of MBSs in the traditional HetNet are the same as those in the cache-enabled HetNet, by substituting (F.4) with $k = 1$ and $\mathbf{q}_1 = \mathbf{q}_2 = \mathbf{1}$ into (F.3) and furthering considering (F.2) and (F.1), we can obtain

$$\mathbb{E}[R_1] = \frac{W M_1}{\mathcal{P}_1} \int_0^\infty \left(\sum_{j=1}^2 \lambda_{j1} (P_{j1} B_{j1})^{\frac{2}{\alpha}} (p_{a,j} Z_{1,j1}(e^x - 1) + 1) \right)^{-1} dx \quad (\text{I.3})$$

Upon substituting (I.3) and (I.1) into (4), Proposition 4 can be proved.

APPENDIX J: PROOF OF COROLLARY 6

Similar to the derivation of Colloary 4, by approximating $Z_{1,jk}(e^x - 1)$ as (G.1) for $x \in [0, \ln 2)$ and as (G.2) for $x \in [\ln 2, \infty)$, (I.3) and (I.1) can be approximated as

$$\mathbb{E}[R_2] \approx \frac{W}{\mathcal{P}_2} \int_0^{\frac{C_{\text{bh}}}{W}} \left(\sum_{j=1}^2 \lambda_{j2} P_{j2}^{\frac{2}{\alpha}} \right)^{-1} dx = \frac{C_{\text{bh}}}{\mathcal{P}_2 \sum_{j=1}^2 \lambda_{j2} P_{j2}^{\frac{2}{\alpha}}} = C_{\text{bh}} \quad (\text{J.1})$$

$$\begin{aligned} \mathbb{E}[R_1] &\approx \frac{W M_1}{\mathcal{P}_1} \left(\int_0^{\ln 2} \left(\sum_{j=1}^2 \lambda_{j1} P_{j1}^{\frac{2}{\alpha}} \right)^{-1} dx + \int_{\ln 2}^\infty \left(\sum_{j=1}^2 \lambda_{j1} P_{j1}^{\frac{2}{\alpha}} \left(p_{a,j} \frac{\Gamma(1-\frac{2}{\alpha})\Gamma(M_j+\frac{2}{\alpha})}{\Gamma(M_j)M_{j1}^{\frac{2}{\alpha}}} e^{\frac{2x}{\alpha}} + 1 - p_{a,j} \right) \right)^{-1} dx \right) \\ &= W M_1 \left(\ln 2 + \frac{1}{\mathcal{P}_1 K_2} \ln \left(1 + \frac{K_2}{K_1} 4^{-\frac{1}{\alpha}} \right) \right) \end{aligned} \quad (\text{J.2})$$

where $K_1 \triangleq \sum_{j=1}^2 \lambda_{j1} P_{j1}^{\frac{2}{\alpha}} p_{a,j} \Gamma(1 - \frac{2}{\alpha}) \Gamma(M_j + \frac{2}{\alpha}) \Gamma(M_j)^{-1} M_{j1}^{-\frac{2}{\alpha}}$, and $K_2 \triangleq \sum_{j=1}^2 \lambda_{j1} P_{j1}^{\frac{2}{\alpha}} (1 - p_{a,j})$.

Upon substituting (J.1) and (J.2) into (4), Corollary 5 can be proved.

REFERENCES

- [1] D. Liu and C. Yang, "Cache-enabled heterogeneous cellular networks: Comparison and tradeoffs," in *Proc. IEEE ICC*, 2016.
- [2] —, "Optimal content placement for offloading in cache-enabled heterogeneous wireless networks," in *Proc. IEEE GLOBECOM*, accepted, 2016.

- [3] N. Bhushan, J. Li, D. Malladi, R. Gilmore, D. Brenner, A. Damnjanovic, R. T. Sukhavasi, C. Patel, and S. Geirhofer, "Network densification: the dominant theme for wireless evolution into 5G," *IEEE Commun. Mag.*, vol. 52, no. 2, pp. 82–89, Feb. 2014.
- [4] V. Chandrasekhar, J. Andrews, and A. Gatherer, "Femtocell networks: a survey," *IEEE Commun. Mag.*, vol. 46, no. 9, pp. 59–67, Sept. 2008.
- [5] S. Woo, E. Jeong, S. Park, J. Lee, S. Ihm, and K. Park, "Comparison of caching strategies in modern cellular backhaul networks," in *Proc. ACM MobiSys*, 2013.
- [6] N. Golrezaei, K. Shanmugam, A. G. Dimakis, A. F. Molisch, and G. Caire, "Femtocaching: Wireless video content delivery through distributed caching helpers," in *Proc. IEEE INFOCOM*, 2012.
- [7] E. Bastug, M. Bennis, and M. Debbah, "Living on the edge: The role of proactive caching in 5G wireless networks," *IEEE Commun. Mag.*, vol. 52, no. 8, pp. 82–89, Aug. 2014.
- [8] D. Liu and C. Yang, "Energy efficiency of downlink networks with caching at base stations," *IEEE J. Sel. Areas Commun.*, vol. 34, no. 4, pp. 907–922, Apr. 2016.
- [9] H.-S. Jo, Y. J. Sang, P. Xia, and J. Andrews, "Heterogeneous cellular networks with flexible cell association: A comprehensive downlink SINR analysis," *IEEE Trans. Wireless Commun.*, vol. 11, no. 10, pp. 3484–3495, Oct. 2012.
- [10] E. Bastug, M. Bennis, M. Kountouris, and M. Debbah, "Cache-enabled small cell networks: modeling and tradeoffs," *EURASIP J. on Wireless Commun. and Netw.*, vol. 2015, no. 1, 2015.
- [11] C. Yang, Y. Yao, Z. Chen, and B. Xia, "Analysis on cache-enabled wireless heterogeneous networks," *IEEE Tran. Wireless Commun.*, vol. 15, no. 1, pp. 131–145, Jan. 2016.
- [12] N. Golrezaei, A. F. Molisch, A. G. Dimakis, and G. Caire, "Femtocaching and device-to-device collaboration: A new architecture for wireless video distribution," *IEEE Commun. Mag.*, vol. 51, no. 4, pp. 142–149, Apr. 2013.
- [13] J. Song, H. Song, and W. Choi, "Optimal caching placement of caching system with helpers," in *proc. IEEE ICC*, 2015.
- [14] B. Blaszczyszyn and A. Giovanidis, "Optimal geographic caching in cellular networks," in *proc. IEEE ICC*, 2015.
- [15] Y. Cui, D. Jiang, and Y. Wu, "Analysis and optimization of caching and multicasting in cache-enabled wireless networks," *IEEE Trans. Wireless Commun., early access*, 2016.
- [16] J. Rao, H. Feng, C. Yang, Z. Chen, and B. Xia, "Optimal caching placement for D2D assisted wireless caching networks," in *Proc. IEEE ICC*, 2016.
- [17] L. Breslau, P. Cao, L. Fan, G. Phillips, and S. Shenker, "Web caching and Zipf-like distributions: Evidence and implications," in *Proc. IEEE INFOCOM*, 1999.
- [18] N. Jindal, J. Andrews, and S. Weber, "Multi-antenna communication in ad hoc networks: Achieving MIMO gains with SIMO transmission," *IEEE Trans. Commun.*, vol. 59, no. 2, pp. 529–540, Feb. 2011.
- [19] Y. S. Soh, T. Quek, M. Kountouris, and H. Shin, "Energy efficient heterogeneous cellular networks," *IEEE J. Sel. Areas Commun.*, vol. 31, no. 5, pp. 840–850, May 2013.
- [20] S. Boyd and L. Vandenberghe, *Convex optimization*. Cambridge university press, 2004.
- [21] TR 36.814 V1.2.0, "Further advancements for E-UTRA physical layer aspects (release 9)," *3GPP*, Jun. 2009.
- [22] S. Lee and K. Huang, "Coverage and economy of cellular networks with many base stations," *IEEE Commun. Lett.*, vol. 16, no. 7, pp. 1038–1040, July 2012.
- [23] S. Singh, H. Dhillon, and J. Andrews, "Offloading in heterogeneous networks: Modeling, analysis, and design insights," *IEEE Trans. Wireless Commun.*, vol. 12, no. 5, pp. 2484–2497, May 2013.
- [24] A. Jeffrey and D. Zwillinger, *Table of integrals, series, and products*, 6th ed. Academic Press, 2000.